

Project, will be equally shared by both countries.

The experimental part of T-J CAVRP has produced encouraging results. First, it was established that whole HIV-1 *gag* genes from subtype B, CRF01_AE, and SIV could be productively expressed by the recombinant BCG-vector. After optimizing the codon usage for viral antigen expression in mycobacteria, we demonstrated that the expression of the HIV-1 p24 antigen by the recombinant BCG increased more than 20-fold (Kanekiyo *et al.*, 2003). We obtained similar results using recombinant non-replicative vaccinia vector DIs, which productively expressed the Gag proteins from HIV subtype B, CRF01_AE, and SIV (Ishii *et al.*, 2002; Izumi *et al.*, 2003). In small animal experiments, these potential HIV vaccine candidates were shown to effectively induce strong anti-HIV specific CTL responses in mice (Ishii *et al.*, 2002).

The same prime-boost regimen, in which the recombinant BCG bacteria were used first and followed by a boost immunization with the recombinant vaccinia DIs that expressed the same HIV antigens, also showed a strong ability to induce CTL in immunized macaque monkeys (Matsuo *et al.*, 2002). This result was critically important to advance the T-J CAVRP into the preclinical testing stage of the HIV vaccine candidates.

PRECLINICAL EVALUATION OF THE THAILAND-JAPAN AIDS VACCINE CANDIDATES

As part of the research capacity building efforts of the T-J CAVRP, facilities and expertise were collaboratively established in the Sasakawa Memorial Animal Facility Building, Nonthaburi, Thailand, where the HIV vaccines would be evaluated in a hu-PBL-NOD-SCID mouse model. Such a complicated but useful animal model enabled us to demonstrate the capability of our prime-boost regimen to induce the desirable neutralizing antibodies that would be required

in order to protect human vaccinees from HIV/AIDS. In one particular experiment, the IgG fraction collected from HIV-1-positive individuals, which has neutralizing activity *in vitro* checked by the MAG1C5 cell line, inhibited virus growth in hu-PBL-NOD-SCID mice more than 100 times compared to negative controls (Ogura *et al.*, 1996; Okamoto *et al.*, 1997; Okamoto *et al.*, 1998).

Next, we established the macaque monkey HIV/AIDS models using chimeric human-simian immunodeficiency virus (SHIV) that was specifically developed for this project. A panel of challenging SHIV stocks was prepared for the proposed vaccine efficacy studies, including the nonpathogenic SHIV-MN, SHIV-HXB, the pathogenic SHIV-C2/1, and its molecular clone, SHIV-C2/1 KS661 (Shinohara *et al.*, 1999; Sakai *et al.*, 2001). In order to demonstrate the potential vaccine efficacy for candidates with the SHIV model, we constructed new recombinant BCG and non-replicative vaccinia DIs that productively express the SIV *gag* protein to match the SIV *gag* gene in the challenging SHIV viruses. Results showed that the recombinant BCG-vectored and recombinant non-replicative vaccinia virus DIs-vectored SIV Gag vaccines induced strong CTL responses in immunized monkeys, respectively. However, the best immune responses in monkeys were obtained when the two vaccines were used in combination as a prime-boost regimen. When the immunized monkeys were challenged with the pathogenic SHIV-C2/1, the vaccination provided full protection for the monkey hosts from developing simian AIDS (Matsuo *et al.*, 2002). The CD4 T-cell decline in the vaccinated monkeys after the lethal challenge of SHIV, which is the hallmark of simian AIDS as well as AIDS in humans, was prevented. The plasma virus load in the vaccinated monkeys after the SHIV challenge also showed approximately 100- to 1000-fold reductions in comparison with unvaccinated monkeys (Matsuo *et al.*, 2002). Moreover, it was demonstrated that oral administration of the recombinant

BCG-based vaccines with two doses of 80 mg in guinea pigs was sufficient to induce the desired virus-specific cell-mediated immune responses, thus presenting the possibility of using the vaccine candidates orally in humans (Kawahara *et al.*, 2002).

These studies also demonstrated that the proposed prime-boost regimen was safe to use in the non-human primate hosts: no detectable adverse effects resulted from vaccination in any of the immunized monkeys. One of the concerns regarding the use of recombinant BCG in Thailand was possible side effects or reduced efficiency in people who were previously immunized with BCG. A series of animal experiments were conducted to address these issues. We showed that prior immunization with BCG did not affect the induction of HIV p24 antigen-specific cellular immunity in monkeys that were immunized with the recombinant BCG/DIs-based HIV vaccines. However, previous exposure to BCG vaccination in monkeys did seem to reduce Gag-specific cellular immune responses in the immunized monkeys by about 50%.

We believe that the recombinant BCG-based HIV vaccines would be safe to use in Thailand. To date, more than two billion people worldwide have been vaccinated with BCG against TB with a proven safety record. With regard to the use of the recombinant vaccinia virus-based HIV vaccines, we believe that the non-replicative DIs strain presents a safer alternative to the MVA (modified vaccinia Ankara) that is being widely used in HIV-1 vaccine development elsewhere. Like the MVA-based HIV-1 vaccines, the recombinant non-replicative vaccinia virus DIs is capable of efficiently expressing the HIV-1 antigens in mammalian host cells. However, the DIs-based viruses lack the replicative ability in these cells, thus producing no infectious viruses. In contrast, MVA is able to replicate in mammalian cells like BHK and CV-1 following infection (Carroll and Moss, 1997). Although the deleted region in DIs is larger than that of MVA, the structural basis for this

distinction between the DIs virus and MVA is not yet known. It was shown that the DIs virus as a smallpox vaccine failed to induce a skin reaction in inoculated infants and permitted revaccination by another smallpox vaccine strain without complications, demonstrating a safety advantage over the use of MVA as a recombinant vaccinia vector (Fujii and Minamitani, 1968).

In order to assure the safety of the T-J CAVRP candidate vaccines, the pilot products of these vaccines are evaluated in baby monkeys, as well as in adult monkeys. Studies showed that as much as 800 mg of the recombinant BCG-based HIV vaccines by oral administration, or repeated subcutaneous injections of 50 mg of the vaccine, did not cause any detectable adverse effects when compared directly with the standard BCG vaccine (Sukpanichnant *et al.*, Department of Pathology, Faculty of Medicine, Siriraj Hospital, Mahidol University, December 2003, unpublished data). Similar safety experiments are underway to evaluate the recombinant non-replicative vaccinia DIs-based HIV vaccines.

FUTURE PLANS

The above-mentioned first generation candidate vaccine incorporates the *gag* gene only, and does not induce sterile immunity because the immunized monkeys do not suppress primary viremia completely after the SHIV challenge. The *gag* gene product cannot induce neutralizing antibodies that block virus entry. Therefore, introduction of the *env* gene to current constructs may be important to enable the vaccines to prevent both HIV-1 infection and disease progression. Furthermore, the construct of a single *gag* gene would have a restricted range of CTL responder population in which the HLA type is involved. To address these issues, future research may be conducted to improve the capacity and expression level of incorporated HIV-1 *env* genes in rBCG and rDIs.

To improve immunogenicity of the vaccine constructs, antigen expression in BCG or in DIs should be optimized. Regarding rBCG, we have already found that the codon-optimized *gag* p24 gene is expressed at a drastically higher level than the native *gag*; this strategy can be applied to other rBCG constructs to make them more immunogenic (Kanekiyo *et al.*, unpublished data). Such investigations are continuing now through collaboration between Japan and Thailand. These approaches are of particular importance to obtain an HIV vaccine that is highly effective.

ACKNOWLEDGEMENTS. We would like to thank Drs. Bonnie Mathieson, Jorge Flores and Rebecca Sheets, Division of AIDS, National Institute of Allergy and Infectious Diseases (NIAID), National Institutes of Health (NIH), Bethesda, MD, USA; Dr. Bernard Moss, Laboratory of Viral Diseases, NIAID, for their helpful discussions; and Drs. Hidemi Takahashi, and Yohko Nakagawa, Department of Microbiology and Immunology, Nippon Medical School, Tokyo, for their helpful discussions. Japan Science and Technology Corporation, the Organization of Pharmaceutical Safety and Research, the "Panel on AIDS" of the US-Japan Cooperative Medical Science Program, Japan Health Sciences Foundation, and the Japanese Ministry of Health, Labor and Welfare also supported this work. This study was also supported by the AIDS vaccine project in conjunction with Japan Science and Technology Corporation.

REFERENCES

- Albright, A.V., Shieh, J.T., Itoh, T., Lee, B., Pleasure, D., O'Connor, M.J., Doms, R.W., and Gonzalez-Scarano, F. (1999). Microglia express CCR5, CXCR4, and CCR3, but of these, CCR5 is the principal coreceptor for human immunodeficiency virus type 1 dementia isolates. *J Virol* 73:205–213.
- Ananworanich, J., Nuesch, R., Teeratakulpisarn, S., Srasuebku, P., Chuenyam, T., Siangphoe, U., Ungsedhaphand, C., Phanuphak, P., and Ruxrungtham, K. (2003). In vivo cell-mediated immunity in subjects with undetectable viral load on protease inhibitor-based versus non-protease inhibitor-based highly active antiretroviral therapy. *J Acquir Immun Defic Syndr* 32:570–572.
- Ariyoshi, K., Promadej, N., Ruxrungtham, K., and Sutthent, R. (2002). Toward improved evaluation of cytotoxic T-lymphocyte (CTL)-inducing HIV vaccines in Thailand. *AIDS Res. Hum. Retroviruses* 18:737–739.
- Balachandra, K., Matsuo, K., Sutthent, R., Hoisanka, N., Boonsarthorn, N., Sawanpanyalert, P., Warachit, P., Yamazaki, S., and Honda, M. (2002). Characteristic of HIV-1 in V3 loop region based on seroreactivity and amino acid sequences in Thailand. *Asian Pac J Allergy Immunol* 20: 93–98.
- Carroll, M.W. and Moss, B. (1997). Host range and cytopathogenicity of the highly attenuated MVA strain of vaccinia virus: propagation and generation of recombinant viruses in a nonhuman mammalian cell line. *Virology* 238:198–211.
- Chujoh, Y., Matsuo, K., Yoshizaki, H., Nakasatomi, T., Someya, K., Okamoto, Y., Naganawa, S., Haga, S., Yoshikura, H., Yamazaki, A., Yamazaki, S., and Honda, M. (2002). Cross-clade neutralizing antibody production against human immunodeficiency virus type 1 clade E and B' strains by recombinant *Mycobacterium bovis* BCG-based candidate vaccine. *Vaccine* 20: 797–804.
- Fujii, R., and Minamitani, M. (1968). Virus infections with exanthema. *Saishin Igaku* 23:1146–1155. In Japanese.
- Fukada, K., Tomiyama, H., Wasi, C., Matsuda, T., Kusagawa, S., Sato, H., Oka, S., Takebe, Y., and Takiguchi, M. (2002). Cytotoxic T-cell recognition of HIV-1 cross-clade and clade-specific epitopes in HIV-1-infected Thai and Japanese patients. *AIDS* 16:701–711.
- Hamano, T., Sawanpanyalert, P., Yanai, H., Piyaworawong, S., Hara, T., Sapsutthipas, S., Phromjai, J., Yamazaki, S., Yamamoto, N., Warachit, P., Honda, M., and Matsuo, K. (2004). Determination of HIV-1 CRF01_AE *gag* p17 and *env*-V3 consensus sequences for HIV/AIDS vaccine design. *AIDS Res Hum Retroviruses* (in press)
- Ishii, K., Ueda, Y., Matsuo, K., Matsuura, Y., Kitamura, T., Kato, K., Izumi, Y., Someya, K., Ohsu, T., Honda, M., and Miyamura, T. (2002). Structural analysis and application of vaccinia virus DIs strain as a completely replication-deficient viral vector for HIV vaccine. *Virology* 302:433–444.
- Izumi, Y., Ami, Y., Matsuo, K., Someya, K., Sata, T., Yamamoto, N., and Honda, M. (2003). Intravenous inoculation of replication-deficient recombinant vaccinia virus DIs expressing simian immunodeficiency virus *gag* controls highly pathogenic

- simian-human immunodeficiency virus in monkeys. *J Virol* 77:13248-13256.
- Kanekiyo, M., Matsuo, K., Hamatake, M., Yamamoto, N., Honda, M. (2003). Optimization of codon usage confers vigorous expression in recombinant *Mycobacterium bovis* BCG vaccine. Proceedings of the International Symposium on Research and Development of Recombinant BCG and Vaccinia Virus-based HIV Vaccine. Tokyo, Japan; 21-24.
- Kawahara, M., Hashimoto, A., Toida, I., and Honda, M. (2002). Oral recombinant *Mycobacterium bovis* bacillus Calmette-Guerin expressing HIV-1 antigens as a freeze-dried vaccine induces long-term, HIV-specific mucosal and systemic immunity. *Clin Immunol* 105:326-331.
- Kitamura, T., Kitamura, Y., and Tagaya, I. (1967). Immunogenicity of an attenuated strain of vaccinia virus on rabbits and monkeys. *Nature* 215:1187-1188.
- Kitsutani, P. T., Naganawa, S., Shiino, T., Matsuda, M., Honda, M., Yamada, K., Taki, M., and Sugiura, W. (1998). HIV type 1 subtypes of nonhemophilic patients in Japan. *AIDS Res Hum Retroviruses* 14:1099-1103.
- Kusagawa, S., Sato, H., Tomita, Y., Tatsumi, M., Kato, K., Motomura, K., Yang, R., and Takebe, Y. (2002). Isolation and characterization of replication-competent molecular DNA clones of HIV type 1 CRF01_AE with different coreceptor usages. *AIDS Res Hum Retroviruses* 18:115-122.
- Lagranderie, M., Balazuc, A.M., Gicquel, B., and Gheorghiu, M. (1997). Oral immunization with recombinant *Mycobacterium bovis* BCG simian immunodeficiency virus nef induces local and systemic cytotoxic T-lymphocyte responses in mice. *J Virol* 71:2303-2309.
- Matsuo, K., Nakasone, T., Izumi, Y., Ami, Y., Ohsu, T., Hamano, T., Yamamoto, N., Yamazaki, S., and Honda, M. (2002). SIV Gag-expressing recombinant BCG-prime and recombinant vaccinia virus DIs strain-boost regimen evokes protective immune response in monkey. XIV International AIDS Conference; July 2002. Barcelona, Spain. TuOrA1222.
- Nabel, G.J. (2001). Challenges and opportunities for development of an AIDS vaccine. *Nature* 410:1002-1007.
- Naganawa, S., Na Ayuttaya, P.I., Duangchanda, S., Auwanit, W., Warachit, P., Miyamura, K., Yamazaki, S., and Honda, M. (1997). A characteristic change of consensus core motif in the V3 region of HIV type 1 clade B, but not in clade E, in Thailand. *AIDS Res Hum Retroviruses* 13:271-273.
- Ogura, A., Noguchi, Y., Yamamoto, Y., Shibata, S., Asano, T., Okamoto, Y., and Honda, M. (1996). Localization of HIV-1 in human thymic implant in SCID-hu mice after intravenous inoculation. *Int J Exp Pathol* 77:201-206.
- Okamoto, Y., Ogura, A., Shibata, S., Amagai, T., Katsura, Y., Asano, T., and Honda, M. (1997). Simple i.v. inoculation of HIV-1 to Thy/Liv SCID-hu mice induce reproducible HIV infection with narrowing of medulla in human thymic implant. *J Vet Med Sci* 59:259-263.
- Okamoto, Y., Eda, Y., Ogura, A., Shibata, S., Amagai, T., Katsura, Y., Asano, T., Kimachi, K., Makizumi, K., and Honda, M. (1998). In SCID-hu mice, passive transfer of a humanized antibody prevents infection and atrophic change of medulla in human thymic implant due to intravenous inoculation of primary HIV-1 isolate. *J Immunol* 160:69-76.
- Pimtanonthai, N., Kangwanshiratada, O., and Charoenwongse, P. (2003). Serological analysis of human leukocyte antigens-A and -B antigens in Thai patients with nasopharyngeal carcinoma. *J Med Assoc Thai* 86 Suppl 2:S237-S241.
- Ruxrungtham, K., and Phanuphak, P. (2001). Update on HIV/AIDS in Thailand. *J Med Assoc Thai* 84 Suppl 1:S1-S17.
- Ruxrungtham, K., Buranapraditkul, S., Kosonsiriluk, S., Kerdsanti, S., Hansasutha, P., Sirivichaykul, S., Rowland-Jones, S., and Phanuphak, P. (2003). HIV-1 specific cytotoxic T-lymphocytes (CTLs) study. Proceedings of the International Symposium on Research and Development of Recombinant BCG and Vaccinia Virus-based HIV Vaccine. Tokyo, Japan; 43-52.
- Sakai, K., Shinohara, K., Takahashi, E., Izumi, Y., Ami, Y., Sasaki, Y., Nakasone, T., and Honda, M. (2001). Molecular cloning of a pathogenic simian-human immunodeficiency virus for HIV/AIDS monkey model. Sixth International Congress on AIDS in Asia and the Pacific; 2001 Oct 5-10. Melbourne, Australia. Abstract p. 84. *Proc Int Cong AIDS Asia Pacific* 6:84.
- Schultz, A.M., and Bradac, J.A. (2001). The HIV vaccine pipeline, from preclinical to phase III. *AIDS* 15: 8147-8158.
- Shinohara, K., Sakai, K., Ando, S., Ami, Y., Yoshino, N., Takahashi, E., Someya, K., Suzaki, Y., Nakasone, T., Sasaki, Y., Kaizu, M., Lu, Y., and Honda, M. (1999). A highly pathogenic simian/human immunodeficiency virus with genetic changes in cynomolgus monkey. *J Gen Virol* 80:1231-1240.
- Sutthent, R., Sumrangsarp, K., Wirachsilp, P., Chaisilwattana, P., Roongpisuthipong, A., Chaiyakul, P., Nooma, P., Honda, M., and Warachit, P. (2001). Diversity of HIV-1 subtype E in semen and cervicovaginal secretion. *J Hum Virol* 4:260-268.
- Tagaya, I., Kitamura, T., and Sano, Y. (1961). A new mutant of dermivaccinia virus. *Nature* 192: 381-382.

- Vejbaesya, S., Eiermann, T.H., Suthipinititharm, P., Ban-cha, C., Stephens, H.A., Luangtrakool, K., and Chandanayingyong, D. (1998). Serological and molecular analysis of HLA class I and II alleles in Thai patients with psoriasis vulgaris. *Tissue Antigens* 52:389-392.
- Ward, F.E., Tuan, S., and Haynes, B.F. (1995). Analysis of HLA Frequencies in Population Cohorts for Design of HLA-Based HIV Vaccines. In: Korber, B., Brander, C., Walker, B.D., Koup, R., Moore, J.P., Haynes, B.F., and Myers, G. (eds.), *HIV Molecular Immunology Database 1995*, Theoretical Biology and Biophysics Group, Los Alamos National Laboratory, Los Alamos, NM. pp. IV-10-16.
- Weniger, B.G., Takebe, Y., Ou, C.Y., and Yamazaki, S. (1994). The molecular epidemiology of HIV in Asia. *AIDS* 8 Suppl 2:S13-S28.

Inhibiting the Arp2/3 Complex Limits Infection of Both Intracellular Mature Vaccinia Virus and Primate Lentiviruses

Jun Komano,* Kosuke Miyauchi, Zene Matsuda, and Naoki Yamamoto

Laboratory of Virology and Pathogenesis, AIDS Research Center, National Institute of Infectious Diseases, Tokyo 208-0011, Japan

Submitted April 2, 2004; Revised September 6, 2004; Accepted September 13, 2004
Monitoring Editor: Thomas Pollard

Characterizing cellular factors involved in the life cycle of human immunodeficiency virus type 1 (HIV-1) is an initial step toward controlling replication of HIV-1. Actin polymerization mediated by the Arp2/3 complex has been found to play a critical role in some pathogens' intracellular motility. We have asked whether this complex also contributes to the viral life cycles including that of HIV-1. We have used both the acidic domains from actin-related protein (Arp) 2/3 complex-binding proteins such as the Wiscott-Aldrich syndrome protein (N-WASP) or cortactin, and siRNA directing toward Arp2 to inhibit viral infection. HIV-1, simian immunodeficiency virus (SIV), and intracellular mature vaccinia virus (IMV) were sensitive to inhibition of the Arp2/3 complex, whereas MLV, HSV-1, and adenovirus were not. Interestingly, pseudotyping HIV-1 with vesicular stomatitis virus G protein (VSV-G) overcame this inhibition. Constitutive inhibition of the Arp2/3 complex in the T-cell line H9 also blocked replication of HIV-1. These data suggested the existence of an Arp2/3 complex-dependent event during the early phase of the life cycles of both primate lentiviruses and IMV. Inhibiting the HIV-1's ability to activate Arp2/3 complex could be a potential chemotherapeutic intervention for acquired immunodeficiency syndrome (AIDS).

INTRODUCTION

When human immunodeficiency virus type 1 (HIV-1) enters cells, the envelope glycoprotein gp120 binds to CD4 and subsequently CXCR4 or CCR5 and initiates membrane fusion at the cell surface. After the membrane fusion the reverse transcription takes place while the viral core components migrate toward cell nucleus where the proviral DNA integrates into the host cell chromosome. However, the protein-protein interactions during these processes of disassembly/uncoating are the least understood among the whole viral life cycle. Despite historical suggestions that actin plays a role in the early phase of HIV-1 infection, its role remains largely unclear. Early studies used chemical inhibitors of actin, which were broadly active on cell physiology or "nonspecific" (Cudmore *et al.*, 1997; Bukrinskaya *et al.*, 1998; Iyengar *et al.*, 1998). To test for a specific role of actin in the early phase of HIV-1's life cycle, we focused on regulators of actin polymerization. It has now been shown that some bacteria and viruses use cellular actin polymerization to propel themselves within cells (Gruenheid and

Finlay, 2003). The key host proteins in these reactions are actin-related protein (Arp) 2/3 complex and its regulators. We hypothesized that Arp2/3 complex-dependent actin nucleation might be required for efficient infection by primate lentiviruses including HIV-1.

The Arp2/3 complex is a seven-subunit protein complex highly conserved among eukaryotes that nucleates actin filaments from the sides of existing filaments (Higgs and Pollard, 2001; Pantaloni *et al.*, 2001). The Arp2/3 complex distributes throughout the cell but is enriched especially at the cortical layer underneath the plasma membrane through which viruses have to pass to infect cells (Flanagan *et al.*, 2001). The Arp2/3 complex is regulated by both Wiscott-Aldrich syndrome protein (WASP) family of proteins and cortactin (Weaver *et al.*, 2003). The carboxy terminal domain of WASP is called VCA domain (verprolin homology, cofilin homology and acidic subdomains) and is also named the WA domain. Intensive studies had revealed that VCA's ability to bind monomer actin through its V subdomain is critical for actin nucleation (Miki and Takenawa, 1998). The CA subdomain confers to N-WASP its binding ability to the Arp2/3 complex as evidenced by physicochemical assays (Machesky and Insall, 1998; Marchand *et al.*, 2001) and x-ray crystallography and cross-linking experiments (Gournier *et al.*, 2001; Robinson *et al.*, 2001; Zalevsky *et al.*, 2001). Actin polymerization, nucleation, and branching are enhanced in the presence of VCA protein in vitro (Higgs *et al.*, 1999; Machesky *et al.*, 1999; Rohatgi *et al.*, 1999). Expression of the VCA protein sequesters the Arp2/3 complex and displaces it from physiological regulation in vivo (Machesky and Insall, 1998; Machesky *et al.*, 1999; Rozelle *et al.*, 2000; Castellano *et al.*, 2001; Harlander *et al.*, 2003). By expressing in tissue culture cells, the VCA protein has been used successfully as an inhibitor of Arp2/3 complex to study the role of

Article published online ahead of print. Mol. Biol. Cell 10.1091/mbc.E04-04-0279. Article and publication date are available at www.molbiolcell.org/cgi/doi/10.1091/mbc.E04-04-0279.

* Corresponding author. E-mail address: ajkomano@nih.gov.jp.

Abbreviations used: Arp2/3, actin-related protein 2/3; CC, cytochalasin; GFP, green fluorescent protein; HIV-1, human immunodeficiency virus type 1; HSV-1, herpes simplex virus type 1; IMV, intracellular mature virus; MLV, murine leukemia virus; RLU, relative light unit; SIV, simian immunodeficiency virus; VSV-G, vesicular stomatitis virus G protein; VV, vaccinia virus; WASP, Wiscott-Aldrich syndrome protein.

Arp2/3 complex in many biologic processes (Zhang et al., 1999; Krause et al., 2000; May et al., 2000; Moreau et al., 2000; Rozelle et al., 2000; McGee et al., 2001; Zhang et al., 2002).

Another Arp2/3 complex regulator is cortactin, a filamentous actin-associated protein originally identified as a substrate of Src (Weed and Parsons, 2001) that is also implicated in the phagocytosis of several invasive bacteria (Dehio et al., 1995; Fawaz et al., 1997; Cantarelli et al., 2000). Cortactin binds directly to the Arp2/3 complex through its amino-terminal acidic domain, NTA, and activates it (Weed et al., 2000; Uruno et al., 2001; Weaver et al., 2001). The NTA protein, like VCA, can serve as an inhibitor of Arp2/3 complex.

We explored the possible involvement of Arp2/3 complex in the early phase of life cycle of primate lentiviruses. In parallel, we tested different virus species including adenovirus, herpes simplex virus type 1 (HSV-1), Moloney murine leukemia virus (MLV), and intracellular mature vaccinia virus (IMV), all of which were reported to use the actin cytoskeleton to infect cells; however, the physical properties and mechanisms of their entry vary (Rosenthal et al., 1985; Kizhatil and Albritton, 1997; Bukrinskaya et al., 1998; Iyengar et al., 1998; Li et al., 1998). We also tested whether changing retroviral envelopes, which forces viruses to enter through different routes, affected the efficiencies of viral entry.

MATERIALS AND METHODS

Cells and Viruses

Human embryonic kidney (HEK) 293 cells and Chinese hamster ovary (CHO)-K1 cells were maintained in Dulbecco's modified Eagle's medium (DMEM, Sigma, St. Louis, MO) supplemented with 10% FBS (Hyclone, Logan, UT), penicillin, and streptomycin (Invitrogen, Carlsbad, CA). H9 cells were maintained in RPMI1640 (Sigma) supplemented with 10% FBS, penicillin, and streptomycin. All the mammalian cell lines were incubated at 37°C in the humidified 5% CO₂ atmosphere. Replication incompetent HIV-1 (HXB2 Δ pr, Δ env, Δ nef) was produced by transfecting the proviral DNA carrying renilla luciferase in place of *nef* open reading frame into 293 T-cells along with the expression plasmid for *env*, *tat*, *rev* and *nef* (pIIIex). When pseudotyping HIV-1, *rev* expressing plasmid and either ecotropic MLV envelope (Ragheb and Anderson, 1994) or vesicular stomatitis virus G (VSV-G) expressing plasmid (Clontech, Palo Alto, CA) were cotransfected with the proviral DNA of HIV-1. HXB2 was used for the replication competent HIV-1. The virus was prepared by transfecting the proviral DNA into 293 T-cells, and the supernatants were collected at 2 d posttransfection. SIV (Δ nef) encoding firefly luciferase in place of *nef* open reading frame was created based on the IL-2-carrying molecular clone of SIVmac239 (Gundlach et al., 1997; kindly provided by Dr. K. Mori). SIV was prepared by transfecting the proviral DNA into COS7 cells, and the supernatants were collected. MLV was produced by transfecting pCMMP LacZIRESGFP, pCMMP eGFP (generous gift from Dr. J. Young), pCMMP GFP-VCA, or pQcLIN (Clontech) into 293 cells along with *gag/pol* and either ecotropic, amphotropic *env*, or VSV-G-expressing plasmids (Ragheb and Anderson, 1994). HSV-1 (KOS) *Rid1/tk12* encoding beta-galactosidase under the regulation of the immediate early promoter ICP4, vaccinia virus encoding T7 RNA polymerase (vTF7.3), and adenovirus type 5 expressing T7 RNA polymerase were generous gifts from Drs. Spear (Dean et al., 1994), Moss (Fuerst et al., 1986), and Ishii (Aoki et al., 1998), respectively, and were prepared according to the previous publications. Adenovirus, HSV-1 and IMV were titrated by the plaque assay using HEK293 or Hela cells; MLV by counting reporter-positive HEK293 cells after 2 to 3 d postinfection, and HIV-1, VSV-G HIV-1, and SIV by using the indicator cells that expressed beta-galactosidase or GFP upon infection. The p24 concentration of eco HIV-1 was adjusted to that of HIV-1 (~100 ng/ml). The neutralization assay using the antibody 2D5 that inhibits infection of IMV but not that of EEV (Ichihashi and Oie, 1996) revealed that 99.4% of our vaccinia virus preparation contained intracellular mature virus (IMV).

Plasmids

The VCA domain (amino acid 392–505) of N-WASP was amplified by PCR from N-WASP cDNA kindly provided by Dr. Takenawa (Miki et al., 1996) with the following primers: VCA sense 5'-CAATTGCGCTTCGATGGGGACCATCAGG-3' and 5'-AAGCTTCAGTCTCCCACTCATCATC-3'. The PCR product was subcloned into pCR4 Blunt TOPO (Invitrogen), sequenced, digested with *MfeI* and *EcoRI*, and cloned into *EcoRI* site of pEGFP-C2 (Clontech), generating pGFP-VCA.

Following two primers, 5'-AGATCTTAGTGGCTGATGGCCAAGAGTCCACACC-3' and 5'-CAATGTGAGTCTCCCACTCATCATC-3', were used to amplify the CA domain (amino acid 470–505) of N-WASP. The PCR fragment was cloned into *BglIII-EcoRI* sites of pEGFP-C2, giving rise to pGFP-CA. GFP-A expression plasmid was generated by annealing following two oligonucleotides and cloned it into the *BglIII-EcoRI* sites of pEGFP-C2: 5'-GATCGATGAAGATGAAGATGAAGATGATGAAGAAGATTTTGGAGATGATGATGATGGGAAGACTGA-3' and 5'-AATTTGAGTCTCCCACTCATCATCTCCTCAAAAATCTTCTCATCTCATCTTTCATCTTCATC-3'. Following oligonucleotides were annealed and ligated into the *BglIII* site of pGFP-VCA giving rise to pGFP-VCA*: 5'-GATCTAGATAACTGATCGGGCGCCG-3' and 5'-GATCGGGCGCCGCATCAGTTATCTA-3'. The NTA domain (amino acid 1–84) of cortactin and Arp2 were amplified by PCR from 293T cDNA with following primers: NTA sense 5'-GGATCTCGAGATGTGGAAAGCTTCAGCAGGCCAC-3', NTA antisense 5'-CAATTGTCAATAGCCATGGGAAGCTTTTGGTCC-3'; Arp2 sense 5'-GGATCTCGAGATGGACAGCCAGGGCAGGAAGG-3', Arp2 antisense 5'-CAATTGTATCGAACAGTCCACCAAGTTTC-3'. PCR fragments were cloned into pCR4 Blunt TOPO, and the *BamHI-MfeI* fragments were cloned into *BglIII-EcoRI* sites of pEGFP-C2, generating pGFP-NTA and pGFP-Arp2. pCMMP GFP-VCA was generated by digesting pCMMP GFP with *AgeI* and *BamHI*, ligated with *AgeI-BamHI* fragment from pGFP-VCA. Transfection efficiencies were measured by pHRL/CMV (Promega, Madison, WI) or pHIV-1 LTR-GFP-Luciferase. F10, the ecotropic MLV receptor from rat, expression plasmid was created by digesting pCDNA F10-*ecoR* (Takase-Yoden and Watanabe, 1999) with *NaeI* followed by the self-ligation. The human nectin 1 alpha (HigR) expression plasmid was generated by inserting *EcoRI* fragment of pEF-806 human nectin 1 alpha 3xFLAG (Sakisaka et al., 2001) into *EcoRI* site of pCDNA3 (Invitrogen). The *XhoI-NotI* fragment of either pCMG3neoCD4 or pCMG3neoCCRS (a generous gift from Dr. Yamashita) was cloned into *XhoI-NotI* sites of pCDNA3 (Invitrogen), generating pCD4 and pCCRS, respectively. The *SnaBI-NotI* fragment from pCCRS was cloned into pMACS4ires (Miltenyi Biotec, Bergisch Gladbach, Germany), generating pCCRS IRES CD4. The CD4 lacking the cytoplasmic tail was amplified by the following primers: 5'-GGATCCCGGGCCACCATGACCCGGGAGTCCCTTTTAGGC-3' and 5'-GAATTCGTGGCCGACACAGAGAAGATGCC-3'. The *XhoI-EcoRI* fragment was cloned into the *AgeI-EcoRI* sites of pEGFP-C2, generating pCD4Acyt. The T7 RNA polymerase (T7 RNAP) expression plasmid pCMMP T7RNAP IRES GFP was created by inserting *XhoI-EcoRI* fragment from pVR1-T7 into *AgeI-MfeI* sites of pCMMP IRES GFP (Aoki et al., 1998). The T7RNAP reporter plasmid pTMBLuci was described previously (Aoki et al., 1998). The following pairs of oligonucleotides were annealed and cloned into *ApaI-EcoRI* sites of pSilencer 1.0-U6 (Ambion, Austin, TX) to generate siRNA expressing vectors directing against GFP and Arp2: GFP sense 5'-GCTGACCCCTGAAGTTCATCTCAAGAGAGATGAACITCAGGGTCAGCTTTTTT-3' and GFP antisense 5'-AATTAAGAAAGCIGACCCITGAAGTTCATCTCTTGAAGATGAACITCAGGGTCAGCGCCG-3'; Arp2 sense 5'-CAGCTTCTTACAGAACGAGTTCAGAGACATCGTCTTAAGTAAAGCITGTTTTT-3' and Arp2 antisense 5'-AATTAAAGAACCTTACITAGAACGAGTCTCTTGAACCTCGTCTTAAGTAAAGCTGGGCC-3'.

Transfection, Magnetic Selection, and Infection

Plasmid DNAs were transfected into cells by using either lipofectamin/lipofectamin plus reagent (Invitrogen) or X-tremeGENE siRNA transfection reagent (Roche Diagnostics, Mannheim, Germany) according to the manufacturer's protocol. The latter reagent, with which the transfection efficiencies reached >90% in 293 cells, was specifically used for preparing samples to carry out Western blot analysis demonstrating the reduction of Arp2 levels. In brief, cells were fed in 48-well plates 1–2 d before transfection. Cells were approximately in 50–60% confluency at transfection. After transfection, cells were trypsinized and plated onto 96-well plates. Transfected cells were magnetically selected by using MACS system directing toward CD4 (Miltenyi Biotec). Cells were infected with viruses of ~0.1–0.5 multiplicity of infection by incubating in the virus-containing culture medium at 37°C for 1–4 h.

Cell-to-cell Fusion Assay

The fusion assay was based on the T7RNAP transcription-dependent reporter assay originally described by Nussbaum et al. (1994), modified versions by Sakamoto et al. (2003). In brief, the T7RNAP "donor" cells were generated by transfecting 293 cells with both T7RNAP and HIV-1's Env expression vectors. The T7RNAP "acceptor" cells were generated by transfecting 293 cells with the T7RNAP reporter (pT7-IRES-Luciferase) along with either CD4 or CD4Acyt, GFP or GFP-VCA, and the renilla luciferase expression vectors. At 48 h posttransfection, these cells were cocultivated for 24 h and lysed in the passive lysis buffer to carry out the dual luciferase assay (Promega).

Detection of Fluorescent Signals

The transfected 293 cells were fixed by 4% formaldehyde in PBS at 48 h posttransfection and imaged by using confocal microscopy META 510 (Carl Zeiss, Jena, Germany). For the images showing pseudopodial extensions, images of different focal planes were projected to generate a single image. The transfected H9 cells were imaged similarly at 48 h posttransfection without fixation. The light transmission image was merged with the green fluorescent signal. Alternatively, the transfected cells were analyzed by the flow cytometry (FACS calibur, Becton Dickinson, San Jose, CA).

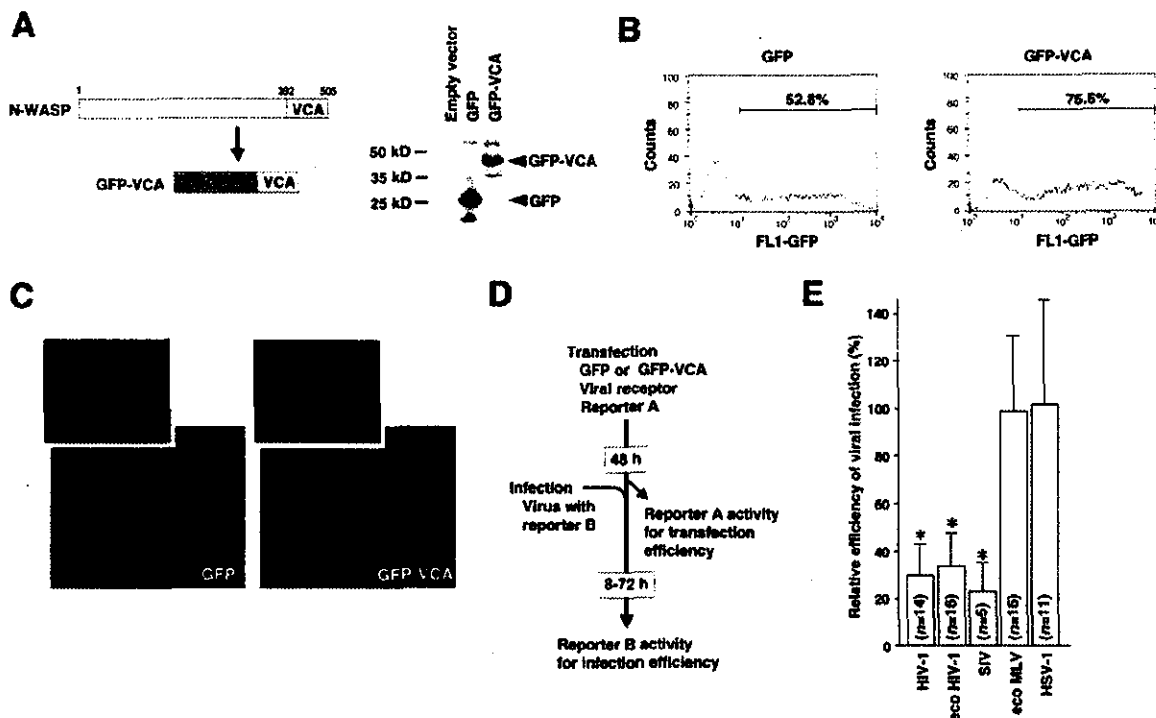


Figure 1. Inhibiting the Arp2/3 complex limited the entry of primate lentiviruses. (A) The carboxy-terminus of N-WASP, VCA domain, was fused to GFP to give rise GFP-VCA. Western blot analysis detected the 41-kDa band, the predicted mol wt for GFP-VCA. (B) The green fluorescence profiles of 293 cells transfected with either GFP or GFP-VCA expression vector were similar to each other as measured by the flow cytometric analysis. (C) GFP-VCA preferentially distributed evenly throughout the cytoplasm. The pseudopodial extension was less active when GFP-VCA was expressed in 293 cells compared with GFP (magnification, $\times 200$; inset, $\times 400$). (D) The experimental procedure was drawn schematically. (E) The relative infection efficiencies of HIV-1, HIV-1 pseudotyped with ecotropic MLV envelope (eco HIV-1), and SIV into cells expressing GFP-VCA were significantly decreased, whereas those of ecotropic MLV (eco MLV) and HSV-1 were not (asterisk, $p < 0.01$). The data represent the average and SD of indicated number of independent experiments.

Western Blot Analysis

Cells were washed with PBS and lysed in a buffer containing 4% SDS, 100 mM Tris-HCl (pH 6.8), 12% 2-ME, 20% glycerol, and bromophenol blue. Samples were boiled for 10 min. Protein lysates approximately equivalent to 5×10^4 cells were separated in SDS-PAGE (Perfect NT Gel, DRC, Tokyo, Japan), transferred to a polyvinylidene fluoride (PVDF) membrane (Immobilon-P⁶⁰, Millipore, Bedford, MA), and blocked with 5% dried nonfat milk (Yuki-Jirushi, Tokyo, Japan) in PBS. For the primary antibody, we used anti-Arp2 antibody H-84 (Santa Cruz Biotechnology, Santa Cruz, CA), antiactin antibody MAB1501 (Chemicon, Temecula, CA), or either an mAb or a polyclonal rabbit antiserum against GFP (Clontech). For the secondary antibody, either a biotinylated anti-mouse antibody (Amersham Pharmacia Biotech, Piscataway, NJ) or a biotinylated anti-rabbit antibody was used. For the tertiary probe, a horseradish peroxidase (HRP)-conjugated streptavidin (Amersham Pharmacia Biotech) was used. Signals were developed by incubating blots with the chemiluminescent HRP substrate (Amersham Pharmacia Biotech) and detected by using Lumi-Imager F1 (Boehringer Mannheim, Mannheim, Germany).

Reporter Assays

Cells were lysed in the Passive Lysis Buffer (Promega) and the dual luciferase assay was performed to measure both firefly and renilla luciferase activities according to the manufacturer's protocol (Promega). The beta-galactosidase activity was measured by using the LumiGal assay kit according to the manufacturer's protocol (Clontech). The chemiluminescence was detected by Lmax (Nihon Molecular Devices, Tokyo, Japan).

ELISA

The amount of p24 antigen of HIV-1 in the culture supernatants was quantified by using Retro TEK p24 antigen ELISA kit according to the manufacturer's protocol (Zepto Metrix, Buffalo, NY). The signals were measured by Vmax ELISA reader (Nihon Molecular Devices).

Statistical Analysis

The significance of differences was tested by one-way analysis of variance (ANOVA) and Student's *t* test. *P* values < 0.05 were considered to be significant.

RESULTS

GFP-VCA Inhibits Infection of Primate Lentiviruses

We first tested whether the viral infection was affected by expressing a potential inhibitor of the Arp2/3 complex GFP-VCA, the VCA domain of N-WASP fused to GFP (Figure 1A). The expression of GFP-VCA protein was verified by Western blot analysis (Figure 1A). The expression levels of GFP-VCA were similar to those of GFP as measured by the flow cytometric analysis at 48 h posttransfection (Figure 1B). GFP-VCA preferentially distributed to the cytoplasm and inhibited the pseudopodial extension compared with GFP alone in agreement with the previous report (Rozelle *et al.*, 2000; Figure 1C). To exclude the possibility that GFP fusion proteins negatively affects the cell surface expression of membrane proteins, we confirmed that the distribution and the levels of transiently and constitutively expressed CD4 and CXCR4 on the cell surface were similar in both GFP- and GFP-VCA-expressing cells as assessed by both confocal microscopy and the flow cytometric analysis (unpublished data).

To evaluate the contribution of the Arp2/3 complex on the viral infection, we used a transient transfection/infection

Table 1. Viruses tested in the receptor-dependent infection system

Virus	Virally encoded reporter	Reporter to normalize infection efficiency	Replication-competency	Infected cells harvested (h postinfection)	Receptor used in this study	S/N ratio ^a
HIV-1	Renilla luciferase	Firefly luciferase	Incompetent	48–72	CD4	4.5
eco HIV-1	Renilla luciferase	Firefly luciferase	Incompetent	48–72	F10	41.2
SIV	Firefly luciferase	Renilla luciferase	Competent	48	CD4 and CCR5	26.4
eco MLV	β -galactosidase	Firefly luciferase	Incompetent	48–72	F10	20.8
HSV-1	β -galactosidase	Firefly luciferase	Competent	8	HigR	207.4

See Figure 1.

^a The signal-to-noise ratio was calculated by dividing the virally encoded reporter gene activities in the GFP-expressing cells by the background signal. Data from all the trials shown in Figures 1 and 4 were averaged.

system in which target cells were transfected with a mixture of plasmid DNA expressing 1) an Arp2/3 complex inhibitor GFP-VCA, 2) a viral receptor, and 3) a reporter gene to normalize transfection efficiencies (depicted in Figure 1D). Because of the nature of cotransfection, the majority of cells uptook the expression vector for GFP-VCA were transfected with the other plasmids because the mixture of DNA contained fivefold excess amount of the GFP-VCA expressing plasmid. At 48 h posttransfection, a portion of transfected cells were collected to measure the transfection efficiencies and others were challenged by a virus expressing a reporter gene to monitor the efficiency of infection. Various times after infection, cells were lysed and the virally encoded reporter gene activities were measured, which was divided by the transfection efficiencies to normalize. Infection of viruses was restricted to the transfected cells by using viral receptors: human CD4 for HIV-1, human CD4 and CCR5 for SIV, F10 for ecotropic MLV envelope-pseudotyped HIV-1 (eco HIV-1) and ecotropic MLV (eco MLV), human nectin-1 alpha (HigR) for HSV-1. Viruses, receptors, and the combination of reporter genes for each virus were summarized in Table 1. Primarily we targeted HEK293 cells because actin cytoskeletal system is shared among eukaryotes. To monitor HSV-1 infection, CHO-K1 cells were used that lack entry molecules for HSV-1. To monitor the efficiencies of single-round viral infection, we used replication-incompetent HIV-1 and MLV. Alternatively, cells infected with replication-competent viruses were lysed at time points before viruses entered the second replication cycle, except SIV, which required 48 h to give sufficient signal to be detected. Importantly, all the viruses tested in this study were reported to utilize actin cytoskeleton to infect cells as examined by using chemical inhibitors against actin such as cytochalasin (CC; Rosenthal *et al.*, 1985; Kizhatil and Albritton, 1997; Bukrinskaya *et al.*, 1998; Iyengar *et al.*, 1998; Li *et al.*, 1998). The infection efficiencies of viruses into cells expressing GFP were set at 100% throughout the study unless stated and the infection efficiencies into GFP-VCA-expressing cells relative to GFP-expressing cells were calculated. For example, when eco HIV-1 was tested, the firefly luciferase activities representing the transfection efficiencies for GFP- and GFP-VCA-transfected cells were 2,065 and 1,854 relative light unit (RLU), respectively, where the background signal was 3 RLU. The renilla luciferase activities reflecting the infection efficiencies into GFP- and GFP-VCA-transfected cells were 4,018 and 1,254 RLU, respectively, where the background was 15 RLU. In this case, the relative infection efficiency of eco HIV-1 into GFP-VCA expressing cells was 34.4%. The relative infection efficiency was introduced be-

cause we were able to integrate data from independent experiments. Results from the indicated number of independent experiments were summarized in Figure 1E. Expression of the GFP-VCA significantly reduced the relative infection efficiencies of HIV-1, eco HIV-1, and SIV (30.3, 35.8, and 22.7%, respectively; $p < 0.01$; Figure 1E), whereas those of eco MLV and HSV-1 (98.5 and 103.5%, respectively; Figure 1E) did not. A 10-fold higher or lower titer of HSV-1 did not affect the results (unpublished data). Consistent with this, the average signal-to-noise ratio did not correlate with the efficiency of inhibition (Figure 1E and Table 1). The GFP-VCA did not inhibit eco MLV but did inhibit the infection of eco HIV-1, suggesting that GFP-VCA's ability to inhibit the infection of eco HIV-1 was eco *env*-independent. It also suggested that the cell surface expression of the F10 was not affected by GFP-VCA expression. In addition, our SIV clone did not encode *nef* and HIV-1 *vpr*, demonstrating that both *nef* and *vpr* were not necessary for primate lentiviruses (HIV-1 and SIV) to infect GFP-VCA-expressing cells efficiently. These results suggested that inhibiting the Arp2/3 complex by GFP-VCA negatively affected the infection of primate lentiviruses.

HIV-1 Pseudotyped with VSV-G Overcomes the Block of Infection by GFP-VCA

To gain insight of the mechanism of GFP-VCA's action to limit primate lentiviral infection, we tested whether the GFP-VCA blocked infection of VSV-G-pseudotyped HIV-1 (VSV-G HIV-1). HIV-1 enters cells by inducing the virus-cell membrane fusion at the cell surface. When HIV-1 was pseudotyped with VSV-G, the route of viral entry became endocytosis (Stein *et al.*, 1987; Maddon *et al.*, 1988). We transfected 293 cells with GFP- or GFP-VCA-expressing plasmid along with one-tenth amount of CD4- and F10-expressing plasmids. Then we enriched transfected cells by using magnetic beads directing toward CD4 at 36–42 h posttransfection. This allowed us to measure the infection efficiencies into the transfected cells only (depicted in Figure 2A). More than 90% of the magnetically selected cells were green fluorescence-positive as examined by the flow cytometric analysis (unpublished data). At 48 h posttransfection, cells were infected either with HIV-1, eco HIV-1 or VSV-G HIV-1. For a comparison, amphotropic MLV (ampho MLV) and VSV-G pseudotyped MLV (VSV-G MLV) were tested in parallel. Infected cells were lysed at 2–3 d postinfection, and the virally encoded reporter gene activities were measured to estimate the relative infection efficiencies (depicted in Figure 2A). For example, when eco HIV-1 was tested in parallel with VSV-G HIV-1, the renilla luciferase activities representing the infection efficiencies of eco HIV-1 into mag-

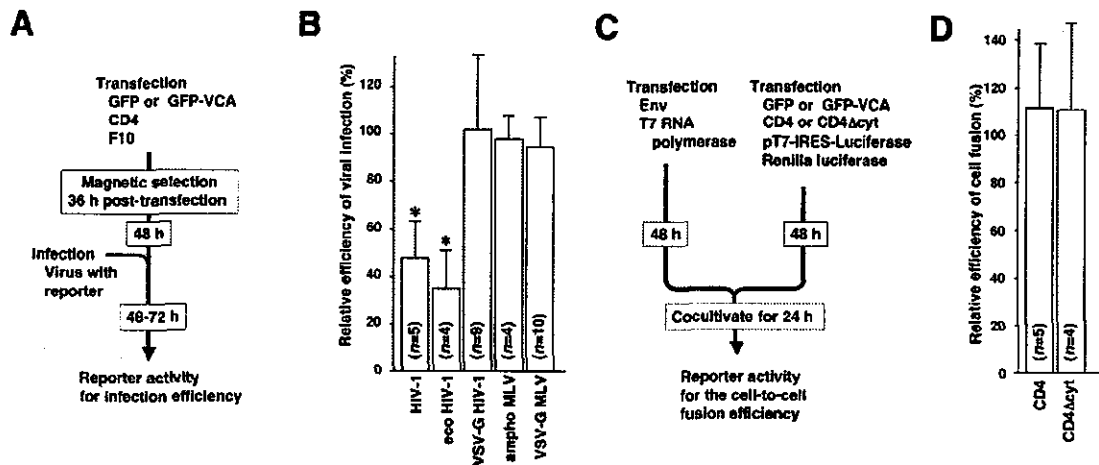


Figure 2. GFP-VCA does not inhibit the infection efficiency of HIV-1 pseudotyped with VSV-G or the membrane fusion induced by the HIV-1's *Env*-CD4 interaction. (A) The experimental procedure using the magnetic selection was drawn schematically. (B) The relative infection efficiencies of HIV-1 and HIV-1 pseudotyped with ecotropic MLV envelope (eco HIV-1) were significantly decreased (asterisk, $p < 0.01$). In contrast, the VSV-G-pseudotyped HIV-1 (VSV-G HIV-1) entered GFP-VCA-expressing cells as efficient as GFP-expressing cells similar to amphotropic MLV (ampho MLV) and VSV-G-pseudotyped MLV (VSV-G MLV). (C) The experimental procedure for the cell-to-cell fusion assay was drawn schematically. (D) GFP-VCA did not negatively affect the cell-to-cell fusion mediated by HIV-1's *Env* and either the full-length CD4 or the CD4 without the cytoplasmic tail (CD4 Δ cyt) compared with GFP. The data represent the average and SD of indicated number of independent experiments.

netically selected GFP- and GFP-VCA-expressing cells were 41,968 and 10,117 RLU, respectively, where the background was 30 RLU. In contrast, the renilla luciferase activities of VSV-G HIV-1-infected cells were 6346 RLU for GFP-expressing cells and 5436 RLU for GFP-VCA-expressing cells where the background signal was 30 RLU. In these cases, the relative infection efficiencies of eco and VSV-G HIV-1 into GFP-VCA-expressing cells were 24.1 and 85.6%, respectively. Results from a number of independent experiments are summarized in Figure 2B. The relative infection efficiencies for HIV-1 and eco HIV-1 were significantly reduced when target cells expressed GFP-VCA compared with GFP alone (47.3 and 36.0%, $p < 0.01$, respectively; Figure 2B). The magnitude of inhibition of HIV-1 infection in this assay was smaller than that of the first experimental setup (Figure 1D), presumably because the levels of CD4 on the cell surface might have decreased after the magnetic selection (Figure 1E). On the other hand, the relative infection efficiency for eco HIV-1 (36.0%, $p < 0.01$; Figure 2B) was similar to the first experimental setup, indicating that the magnetic selection did not detectably influence the cellular

susceptibility to viral infection. Interestingly, VSV-G HIV-1-infected GFP-VCA-positive cells at efficiencies almost equal to GFP-positive cells (101.7%, Figure 2B). Similarly, both ampho MLV- and VSV-G MLV-infected GFP-VCA-expressing cells as efficient as they did GFP-expressing cells (96.9% for ampho MLV, 93.2% for VSV-G MLV; Figure 2B). In this experimental setup, the signal-to-noise ratio of HIV-1 and eco HIV-1 increased compared with the first experimental system; however, the results remained the same (Figures 1E and 2B, and Table 2). These data indicated that the GFP-VCA was unable to block HIV-1 infection when HIV-1 entered cells through the VSV-G-mediated endocytosis. In other words, the reverse transcription, nuclear import, and integration of HIV-1 genome into the host chromosome were able to proceed in the presence of GFP-VCA.

The Efficiency of the Membrane Fusion Is Not Negatively Affected by GFP-VCA

The membrane fusion is the critical event when enveloped viruses infect cells. We next asked if the expression of GFP-

Table 2. Viruses tested in the magnetic selection system

Virus	Virally encoded reporter	Reporter to normalize infection efficiency	Replication-competency	Receptor used in this study	S/N ratio ^a
HIV-1	Renilla luciferase	Firefly luciferase	Incompetent	CD4	7.2
eco HIV-1	Renilla luciferase	Firefly luciferase	Incompetent	F10	101.3
VSV-G HIV-1	Renilla luciferase	Firefly luciferase	Incompetent		251.6
ampho MLV	β -galactosidase	Firefly luciferase	Incompetent		12.0
VSV-G MLV	β -galactosidase	Firefly luciferase	Incompetent		590.4

See Figure 2.

^a The signal-to-noise ratio was calculated by dividing the virally encoded reporter gene activities in the GFP-expressing cells by the background signal. Data from all the trials shown in Figure 2 were averaged.

Table 3. Viruses tested in the T7 RNA polymerase system

Virus	Reporter to normalize infection efficiency	Replication-competency	Infected cells harvested (h postinfection)	S/N ratio ^a
IMV	Renilla luciferase	Competent	3	1808.4
Adenovirus	Renilla luciferase	Competent	24	901.3

See Figure 3.

^aThe signal-to-noise ratio was calculated by dividing the luciferase activities in the GFP-expressing cells by the background signal. Data from all the trials shown in Figures 3 and 4 were averaged.

VCA inhibited the membrane fusion through HIV-1's *Env*-receptor interaction. We carried out the cell-to-cell fusion assay in which *Env*-positive cells expressing T7 RNA polymerase (T7RNAP) were fused to the CD4-positive cells carrying the T7RNAP promoter-driven firefly luciferase reporter plasmid (depicted in Figure 2C). The efficiency of the cell-to-cell fusion was measured by the firefly luciferase activity divided by the renilla luciferase activity representing the transfection efficiency. The ratio of the firefly luciferase to renilla luciferase activities in GFP-expressing cells was set at 100%, and the relative efficiencies of cell-to-cell fusion of GFP-VCA-expressing cells were calculated. It revealed that the efficiencies of cell-to-cell fusion initiated by the interaction between HIV-1's *Env* and CD4 were not inhibited when GFP-VCA was expressed in CD4-expressing cells compared with GFP (114%, Figure 2D).

To eliminate a possibility that the GFP-VCA inhibited the expression/distribution of CD4 on the cell surface, we examined whether the CD4 lacking the cytoplasmic domain (CD4 Δ cyt) was able to support the membrane fusion in the presence of GFP-VCA. Because GFP-VCA distributed throughout the cytoplasm, it was unlikely that the motility of CD4 Δ cyt on the cell surface was restricted by GFP-VCA. It was found that CD4 Δ cyt induced the cell-to-cell fusion in the presence of GFP-VCA at efficiencies almost equal to the full length CD4 (113%, Figure 2D). In support of this, enveloped viruses (HSV-1, MLV, and VSV-G HIV-1) were able to infect GFP-VCA-positive cells as efficient as GFP-positive cells (Figures 1E and 2B). In particular, when HSV-1 and amphi MLV enter cells, like HIV-1, the membrane fusion takes place at the cell surface (Fuller and Spear, 1987; McClure *et al.*, 1990; Wittels and Spear, 1991; Nussbaum *et al.*, 1993). These data indicated that the virus-cell membrane fusion was not inhibited by GFP-VCA. According to the data presented hereby, it seemed likely that GFP-VCA did not negatively affect the expression of receptors or viral attachment to receptors, or the virus-cell membrane fusion. Because VSV-G HIV-1-infected cells in the presence of GFP-VCA, we assume that GFP-VCA inhibits HIV-1's life cycle after the membrane fusion before or at the reverse transcription, especially when HIV-1 enters cells through the membrane fusion at cell surface where the viral core is placed in the cortical compartment.

GFP-VCA Inhibits Infection of Intracellular Mature Vaccinia Virus but Not Adenovirus

To test whether the inhibition of viral entry by GFP-VCA was limited to the primate lentiviruses, we examined both intracellular mature vaccinia virus (IMV) and adenovirus. IMV enters cells via the membrane fusion at cell surface, which is accompanied by a drastic actin cytoskeletal reorganization (reviewed by Smith *et al.*, 2002). Adenovirus infects

cells through clathrin-dependent endocytosis (Wang *et al.*, 1998). Adenovirus was the only envelope-free virus studied in this article. These viruses encoded T7 RNA polymerase as a reporter (Table 3). To detect the infection signal from transfected/infected cells, we introduced the T7 promoter-driven luciferase reporter into 293 cells (Figure 3A). For example, when IMV was tested, the renilla luciferase activities representing the transfection efficiencies for GFP- and GFP-VCA-transfected cells were 485 and 556 RLU, respectively, where the background signal was 8 RLU. The firefly luciferase activities reflecting the infection efficiencies of virus into GFP- and GFP-VCA-transfected cells were 29,020 and 10,044 RLU, respectively, where the background was 23 RLU. In this case, the relative infection efficiency of IMV into GFP-VCA-expressing cells was 30.3%. Results from a number of independent experiments were summarized in Figure 3B. The relative infection efficiency of IMV was significantly reduced (30.6%, $p < 0.01$; Figure 3B), whereas adenovirus-infected GFP-VCA-expressing cells as efficiently as GFP-expressing cells (98.3%, Figure 3B). IMV gave the highest signal-to-noise ratio throughout the study, yet its infection was blocked efficiently by GFP-VCA (Table 3). Considering all the signal-to-noise data, it was suggested that the signal-to-noise ratio did not positively correlate with the magnitude of inhibition of viral infection. Ten-fold higher or lower titer of either IMV or adenovirus did not affect the results

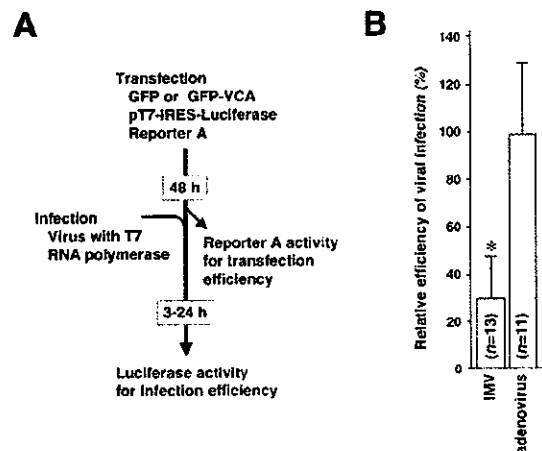


Figure 3. Limiting infection of IMV but not adenovirus by inhibiting the Arp2/3 complex. (A) The experimental procedure was drawn schematically. (B) The significant decrease of relative infection efficiency of IMV, but not adenovirus, was observed (asterisk, $p < 0.01$). The data represent the average and SD of indicated number of independent experiments.

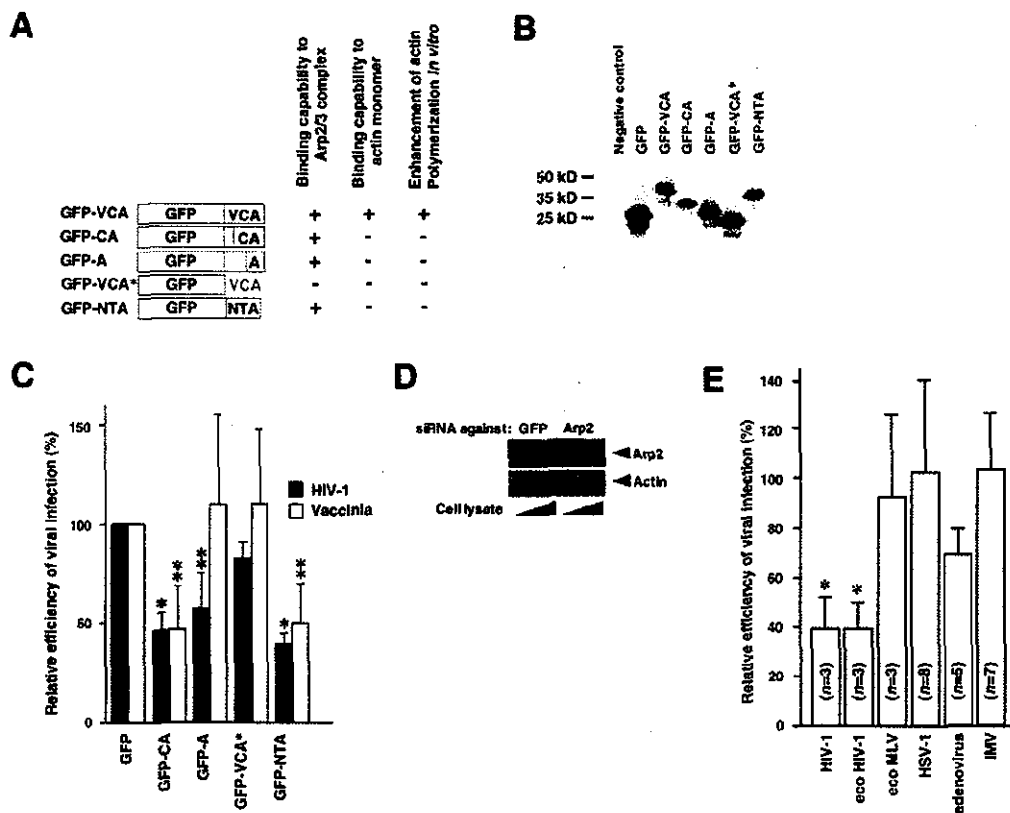


Figure 4. Inhibitory effects of GFP-VCA derivatives, GFP-NTA, and siRNA against Arp2 on the infection of both HIV-1 and IMV. (A) Schematic drawing of GFP-VCA derivatives and GFP-NTA. (B) Western blot analysis detected 30-, 41-, 32-, 30-, 28-, and 37-kDa bands, each predicted mol wt for GFP, GFP-VCA, -CA, -A, VCA*, and -NTA, respectively. (C) The relative infection efficiencies of HIV-1 (■) and IMV (□) were significantly inhibited when cells expressed GFP-CA and GFP-NTA (asterisk, $p < 0.01$; double asterisks, $p < 0.05$). Expression of GFP-A significantly reduced the relative infection efficiency for HIV-1 but not for IMV. GFP-VCA* did not detectably inhibited infection of both viruses. The data represent the average and SD of more than three independent experiments. (D) The siRNA directed against Arp2 down-modulated expression of Arp2 by 73.5% on the average, whereas the expression of siRNA against GFP did not as demonstrated by Western blot analysis in which 293 cell lysates corresponding to the 5×10^4 or 2×10^5 were analyzed at 2 d posttransfection. (E) Introducing siRNA against Arp2 significantly reduced the relative infection efficiencies of HIV-1 and HIV-1 pseudotyped with ecotropic MLV envelope (eco HIV-1; asterisk, $p < 0.01$) but not ecotropic MLV (eco MLV), HSV-1, adenovirus, and IMV. The data represent the average and SD of indicated number of independent experiments.

(unpublished data). These data suggested that inhibiting the Arp2/3 complex by GFP-VCA negatively affected infection of IMV as well as primate lentiviruses. We focused on HIV-1 and IMV for the further studies.

GFP-VCA's Ability to Nucleate Actin Filament Is Not Necessary to Inhibit Viral Entry

We attempted to locate the domain within VCA responsible for the inhibition of HIV-1 and IMV infection. We generated a series of truncated GFP-VCA mutants (Figure 4A). Their functions were also summarized according to the previous reports (Figure 4A; Takenawa and Miki, 2001; Weaver *et al.*, 2003). Expression of each mutant was verified in Western blot analysis (Figure 4B). Introducing a stop codon into GFP-VCA after the GFP open reading frame allowed VCA-encoding RNA to be expressed but not VCA protein (GFP-VCA*). Expression of GFP-VCA* did not inhibit infection of both HIV-1 and IMV (82.9 and 112.6%, respectively; Figure 4C), suggesting that the inhibition of viral entry attributed to the VCA protein, not the VCA-encoding RNA (Figure 4C). GFP-CA retained the ability to limit both HIV-1 and IMV

infection (46.7 and 46.4%, $p < 0.01$ and $p < 0.05$, respectively, Figure 4C). Expression of GFP-A inhibited HIV-1 infection less efficiently than other derivatives (57.7%, $p < 0.05$; Figure 4C). However, GFP-A was unable to limit IMV infection (110.8%, Figure 4C) although synthetic peptides of A subdomain has been shown to retain the binding affinity to the Arp2/3 complex as high as VCA *in vitro* (Panchal *et al.*, 2003). These data suggested that the V subdomain was not required for the inhibition of HIV-1 and IMV infection. It seemed likely that C and A subdomains functioned cooperatively *in vivo* to inhibit infection of both HIV-1 and IMV.

To further verify that the reduction of viral infection efficiencies was due to the inhibition of Arp2/3 complex functions, we have tested whether another potential Arp2/3 complex inhibitor NTA, amino-terminal acidic domain of cortactin (amino acids 1–84), was also able to limit both HIV-1 and IMV infection as did VCA. Cortactin is unrelated to WASP family of proteins but is able to bind the Arp2/3 complex through the NTA domain. Expression of GFP-NTA was verified by Western blot analysis (Figure 4B). As expected, GFP-NTA reduced the infection efficiencies of both

HIV-1 and IMV (39 and 50%, $p < 0.01$ and $p < 0.05$, respectively; Figure 4C). These data confirmed that inhibiting functions of the Arp2/3 complex was indeed responsible for limiting both HIV-1 and IMV infection. As GFP-NTA lacked the ability to nucleate actin filaments similar to GFP-CA and because of the reported functions of CA subdomains (Figure 4A), it was strongly suggested that, not their abilities to enhance actin nucleation, but GFP fusion proteins' abilities to bind the Arp2/3 complex was primarily important to inhibit viral infection.

In addition, we tested whether down-regulating expression of Arp2 by using siRNA technique inhibited both HIV-1 and IMV infection. The GFP-VCA and -NTA were able to inhibit functions of Arp2/3 complex by binding to it directly, whereas siRNA against Arp2 down-modulated expression of Arp2, therefore decreasing the number of Arp2/3 complex. Because siRNA against Arp2 was not able to inhibit the function of preexisting Arp2/3 complex directly, it was expected that siRNA against Arp2 should be able to limit viral infection, if any, less efficiently than GFP-VCA. Transfecting the plasmid vector expressing siRNA directing against Arp2 reduced the expression of endogenously expressed Arp2–26.5% in 293 cells as demonstrated by Western blotting analysis (Figure 4D). Viral infection efficiencies were measured using the experimental setups (Figures 1D and 3A) except the GFP or GFP-VCA expression plasmid was replaced with the siRNA expression vectors against GFP or Arp2. When siRNA directing toward GFP was set as 100%, the relative efficiencies of both HIV-1 and eco HIV-1 infection in cells expressing siRNA against Arp2 became 39.4 and 39.1%, respectively (both, $p < 0.01$; Figure 4E). Adenovirus infection was slightly inhibited by the siRNA against Arp2 (69.4%, Figure 4E). However, the relative infection efficiencies of eco MLV, HSV-1, and IMV were not significantly reduced by siRNA directed toward Arp2 (91.3, 103.8, and 104.4%, respectively, Figure 4E). Given that the other two Arp2/3 inhibitors were able to limit IMV and HIV-1 infection, it seemed reasonable to speculate that the inhibition of HIV-1 infection by siRNA was due to the down-modulation of newly synthesized Arp2. However, we were unable to limit the infection of IMV by siRNA against Arp2. We assumed that this was either because siRNA was unable to down-regulate expression of Arp2, therefore Arp2/3 complex, at levels sufficient to block the entry of IMV or the number of the preexisting Arp2/3 complex might be sufficient to support IMV infection, or both.

HIV-1 Replication Is Negatively Affected When GFP-VCA Is Constitutively Expressed in H9 Cells

Finally, we asked whether the replication of HIV-1 was inhibited in T-cells, one of the natural targets of HIV-1. To do this, we isolated H9 cell clones either expressing GFP or GFP-VCA constitutively by infecting H9 cells with MLV vector followed by the limiting dilution. Introducing expression plasmid for GFP-VCA did not alter the morphology of H9 cells compared with GFP-expressing cells or untransfected cells when observed under the confocal microscopy at 48 h posttransfection (Figure 5A) as well as stable cell clones (unpublished data). H9 GFP-VCA clones proliferated at speed indistinguishable from H9 GFP clones (unpublished data). We verified the expression of GFP and GFP-VCA in isolated clones by Western blot analysis (Figure 5B). However, the average expression levels of GFP-VCA appeared low compared with those of GFP in H9 clones (Figure 5B). We infected six H9-GFP and three H9-GFP-VCA clones with a replication-competent HIV-1 (HXB2) and collected culture supernatants at different time points to monitor the viral

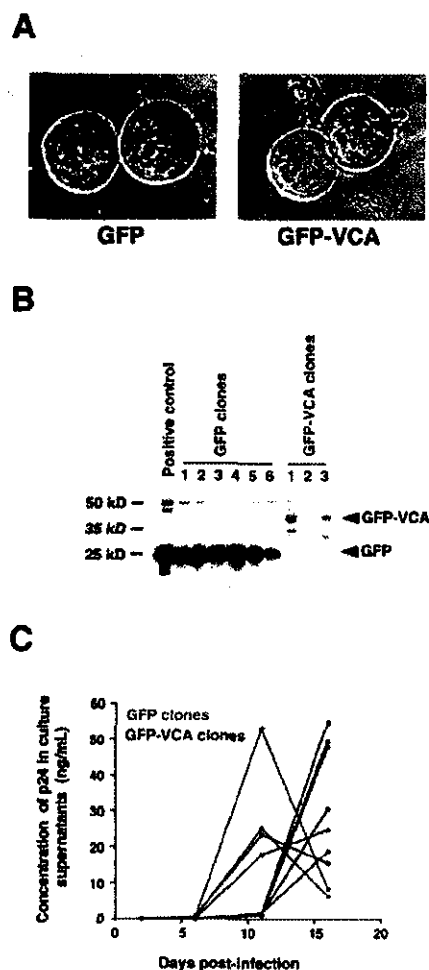


Figure 5. Slow replication kinetics of HIV-1 in H9 cells expressing GFP-VCA constitutively. (A) The morphology of H9 cells was not drastically altered when GFP-VCA was expressed compared with GFP or untransfected cells. The green fluorescent image was merged with the transmission image (magnification, $\times 630$). (B) H9 clones stably expressed GFP or GFP-VCA as demonstrated by Western blot analysis (arrowheads). (C) The amount of p24 antigen in the culture supernatants accumulated rapidly in H9-GFP cell clones (red), whereas H9-GFP-VCA clones did not support the efficient HIV-1 replication (blue). Similar results were obtained by two independent experiments.

replication by measuring the amount of p24 viral antigen. The replication kinetics of HIV-1 in GFP-expressing H9 clones showed a rapid propagation of HIV-1 in culture. In contrast, the amount of p24 in the culture supernatants of H9 GFP-VCA clones did not accumulate, suggesting that the HIV-1 replication was substantially suppressed in H9 GFP-VCA clones (Figure 5C). The replication assay was carried out twice consecutively and similar data were obtained. On the average, the peak of HIV-1 replication kinetics in GFP-VCA clones delayed a week compared with GFP clones. The maximum amount of p24 in the culture supernatants of H9 GFP-VCA clones did not appear different from those of H9 GFP clones.

We next examined whether the viruses propagated in H9 GFP-VCA clones were mutants capable of replicating in the presence of GFP-VCA. We isolated viral RNA from the

culture supernatants of a H9 GFP clone and three H9 GFP-VCA clones and sequenced the *gag/pro/pol* region because the GFP-VCA's ability to limit HIV-1 infection did not depend on *Env*, *Nef*, *Vpr*, and *Rev*. However, we could not find any nucleic acid alterations when the viral sequences from an H9 GFP-VCA culture were compared with the one from an H9 GFP culture. These data suggested that the levels of GFP-VCA in H9 clones might be insufficient to confer the selective advantage for mutant viruses to take over the wild-type HIV-1. We found that the late phase of HIV-1 viral life cycle was slightly affected by GFP-VCA. Transfecting proviral DNA into 293 T-cells along with the expression vector for GFP-VCA yielded fewer amount of p24 antigen in the culture supernatant (72%) compared with GFP alone. Taken together, the decreased replication kinetics of HIV-1 in H9 GFP-VCA was assumed to be mostly due to the inhibition of the early phase, partly the late phase, of HIV-1's life cycle. These data demonstrated that the constitutive inhibition of the Arp2/3 complex by expressing GFP-VCA limited efficient replication of HIV-1 in T-cells as well as epithelial cell systems.

DISCUSSION

We have demonstrated that the Arp2/3 complex contributes to the efficient infection of both primate lentiviruses (HIV-1 and SIV) and IMV but not MLV, HSV-1, and adenovirus. Actin cytoskeleton has been shown to play a role in the infection of all the viruses tested in this study according to previous studies using the chemical actin inhibitor (Rosenthal *et al.*, 1985; Kizhatil and Albritton, 1997; Bukrinskaya *et al.*, 1998; Iyengar *et al.*, 1998; Li *et al.*, 1998; Locker *et al.*, 2000). In addition, the Arp2/3 complex-mediated actin nucleation is sensitive to CC (Welch *et al.*, 1998). Therefore, GFP-VCA's ability to limit infection of primate lentiviruses and IMV might be a part of, if not all, the mechanism by which CC reduced the efficiency of viral infection. In other words, primate lentiviruses and IMV might utilize the Arp2/3 complex-dependent actin polymerization system to support their early phase of viral life cycles. In contrast, MLV, HSV-1, and adenovirus might utilize actin to enter cells in an Arp2/3 complex-independent manner. Perhaps, other functional aspects of actin are important for their efficient infection such as the actin cable-dependent trafficking system. Our data clearly demonstrated that the different viruses use actin system differently. It was reported that the infection of HIV-1 was inhibited by CC at least two different levels: 1) by limiting viral receptor/coreceptor clustering upon viral attachment (Iyengar *et al.*, 1998); and 2) by disrupting establishment of active reverse transcription complex (Bukrinskaya *et al.*, 1998). Our findings suggest a possible involvement of the Arp2/3 complex in the latter process or a presence of another actin polymerization-dependent step between two processes.

What is the molecular mechanism by which the Arp2/3 complex supports infection of both primate lentiviruses and IMV? One of the possibilities is that these viruses may activate the Arp2/3 complex and nucleate actin filaments to support their entry. It has been reported that an acidic motif DDW or DEW can be found among cellular Arp2/3 complex-binding proteins including WASP, cortactin, and MyoD as well as *Listeria monocytogenes* surface protein ActA (Weed and Parsons, 2001). We are unable to find such a binding motif in proteins encoded by both HIV-1 and SIV. Therefore, these viruses may not activate Arp2/3 complex due to a direct interaction between viral gene products and Arp2/3 complex. There are two regulatory pathways known to ac-

tivate the Arp2/3 complex. One is WASP/WAVE pathway and the other being cortactin pathway. Expression of the dominant-negative derivatives of N-WASP, WAVES, and cortactin were unable to limit the infection of both HIV-1 and IMV (unpublished observation, consistent with the Locker's finding, Locker *et al.*, 2000). The dominant-negative derivative of cdc42, RhoGTPase family protein that locates upstream of WASP/WAVE pathway, was also unable to reduce the relative infection efficiencies of both viruses (unpublished observation). These data implied that the activation of Arp2/3 complex upon infection of both lentiviruses and IMV might be mediated by novel virus-host interactions. Inhibiting the Arp2/3 complex by GFP-VCA did not drastically reduce the efficiency of HIV-1 production as did that of HIV-1 infection, suggesting that the incoming HIV-1 might have something unique which budding virus lacks. We speculate that viral gene products cleaved by HIV-1's protease may be responsible to induce activation of Arp2/3 complex because viral protease become active when viral particles are released from cells such that the cleaved proteins are present at high concentrations only in mature virus particles. VV encodes envelope protein A36R that binds adaptor proteins Nck, Wip, Grb2 that recruits and activates WASP-Arp2/3 complex system (Frischknecht *et al.*, 1999; Rietdorf *et al.*, 2001; Scaplehorn *et al.*, 2002). These molecular interactions are known to be important for vaccinia virus to bud from infected cells as extracellular enveloped virus (EEV). However, IMV does not have A36R on its envelope. Accordingly, IMV should initiate activation of Arp2/3 complex via A36R-independent mechanisms.

On the basis of our data as well as previous observations, we propose models in which the Arp2/3 complex plays a role in the entry of both primate lentiviruses and IMV. HIV-1 enters cells via the membrane fusion on the cell surface (Stein *et al.*, 1987; Maddon *et al.*, 1988). The viral core complex is released to the cytoplasm immediately after the membrane fusion over the cortical layer. Our model is that the viral core components, independent of *Env*, *Nef*, *Vpr*, and *Rev*, recruit adaptor proteins and activate the Arp2/3 complex to generate mechanical force by which HIV-1's core complex passes through the cortical layer and migrates toward the nucleus efficiently (Figure 6A). McDonald *et al.* (2002) had shown that the microtubule system supports long-distance movement of HIV-1's core complex. It is possible that lentiviruses utilize the Arp2/3 complex-mediated active transport system to get access to a subcellular compartment where they meet microtubule system. Consistent with our model, a short-distance rapid movement of HIV-1's core was observed in the time-lapse imaging, which suggested a presence of an actin polymerization-dependent transport (McDonald *et al.*, 2002). On the other hand, IMV enters cells via the membrane fusion at the cell surface as suggested by the intensive studies including electron microscopic studies (reviewed in Smith *et al.*, 2002). IMV infection induces the formation of actin-rich cell surface protrusions partly due to GTPase *Rac1* signaling (Locker *et al.*, 2000) and is inhibited by treating cells with CCD (Vanderplasschen *et al.*, 1998; Locker *et al.*, 2000). Taken together, the Arp2/3 complex-mediated actin polymerization may be required for not only the late phase but also the early phase of IMV's life cycle, specifically at the postmembrane fusion processes (Figure 6B). Also, it is necessary to reorganize the cortical actin network to transport the virus-core toward the cytoplasmic subcompartment where the vaccinia virus replicates. The Arp2/3 complex may play a role in the latter process (Figure 6B). In any case, IMV induces relatively global cytoskeletal reorganization in which a substantial

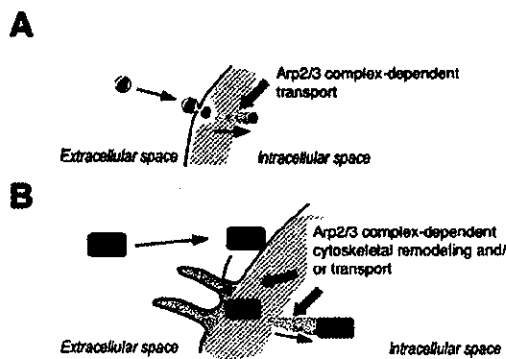


Figure 6. Models in which the Arp2/3 complex supports infection of both primate lentiviruses and IMV. (A) Primate lentiviruses enter cells via membrane fusion at cell surface. After membrane fusion, viral gene products might initiate activation of Arp2/3 complex-dependent actin polymerization (red) behind the viral core to cross the cortical layer (gray). (B) IMV also enters cells via membrane fusion at the cell surface. At or soon after the attachment, the dynamic actin cytoskeletal reorganization takes place that depends partly on the Arp2/3 complex-mediated actin polymerization (red), which may facilitate viral entry. Alternatively, the Arp2/3 complex-mediated actin polymerization (red) powers the viral core (green) to migrate toward the cytoplasmic compartment in which vaccinia virus replicates.

number of Arp2/3 complex should participate. This may account for the less efficient block of IMV's infection by both GFP-A and siRNA directing against Arp2 (Figure 4, C and E).

Our finding suggested a new therapeutic target to control HIV-1 replication in AIDS patients. We should be able to limit HIV-1 replication by inhibiting the HIV-1's ability to activate Arp2/3 complex by a small chemical compound. It is underway to determine which viral gene product is responsible to activate Arp2/3 complex.

ACKNOWLEDGMENTS

We thank Drs. Hironori Sato, Bill Sugden, and Tsutomu Murakami for critical reading of the manuscript and Yuko Futahashi for the technical assistance. We also thank Drs. T. Takenawa, A. Yamashita, J. Young, E. Freed, P. G. Spear, Y. Takai, S. Takase-Yoden, W. Sugiura, and K. Mori for generously sharing reagents and equipments. This work was partly supported by both the Japan Health Science Foundation and a grant from Japanese Ministry of Health, Labor, and Welfare.

REFERENCES

Aoki, Y., Aizaki, H., Shimoike, T., Tani, H., Ishii, K., Saito, I., Matsuura, Y., and Miyamura, T. (1998). A human liver cell line exhibits efficient translation of HCV RNAs produced by a recombinant adenovirus expressing T7 RNA polymerase. *Virology* 250, 140–150.

Bukrinskaya, A., Brichacek, B., Mann, A., and Stevenson, M. (1998). Establishment of a functional human immunodeficiency virus type 1 (HIV-1) reverse transcription complex involves the cytoskeleton. *J. Exp. Med.* 188, 2113–2125.

Cantarelli, V.V., Takahashi, A., Akeda, Y., Nagayama, K., and Honda, T. (2000). Interaction of enteropathogenic or enterohemorrhagic *Escherichia coli* with HeLa cells results in translocation of cortactin to the bacterial adherence site. *Infect. Immun.* 68, 382–386.

Castellano, F., Le Clainche, C., Patin, D., Carlier, M.F., and Chavrier, P. (2001). A WASp-VASP complex regulates actin polymerization at the plasma membrane. *EMBO J.* 20, 5603–5614.

Cudmore, S., Reckmann, I., and Way, M. (1997). Viral manipulations of the actin cytoskeleton. *Trends Microbiol.* 5, 142–148.

Dean, H.J., Terhune, S.S., Shieh, M.T., Susmarski, N., and Spear, P.G. (1994). Single amino acid substitutions in gD of herpes simplex virus 1 confer resistance to gD-mediated interference and cause cell-type-dependent alterations in infectivity. *Virology* 199, 67–80.

Dehio, C., Prevost, M.C., and Sansonetti, P.J. (1995). Invasion of epithelial cells by *Shigella flexneri* induces tyrosine phosphorylation of cortactin by a pp60-src-mediated signalling pathway. *EMBO J.* 14, 2471–2482.

Fawaz, F.S., van Ooij, C., Homola, E., Mutka, S.C., and Engel, J.N. (1997). Infection with *Chlamydia trachomatis* alters the tyrosine phosphorylation and/or localization of several host cell proteins including cortactin. *Infect. Immun.* 65, 5301–5308.

Flanagan, L.A., Chou, J., Falet, H., Neujahr, R., Hartwig, J.H., and Stossel, T.P. (2001). Filamin A, the Arp2/3 complex, and the morphology and function of cortical actin filaments in human melanoma cells. *J. Cell Biol.* 155, 511–517.

Frischknecht, F., Moreau, V., Rottger, S., Gonfoni, S., Reckmann, I., Superti-Furga, G., and Way, M. (1999). Actin-based motility of vaccinia virus mimics receptor tyrosine kinase signalling. *Nature* 401, 926–929.

Fuerst, T.R., Niles, E.G., Studier, F.W., and Moss, B. (1986). Eukaryotic transient-expression system based on recombinant vaccinia virus that synthesizes bacteriophage T7 RNA polymerase. *Proc. Natl. Acad. Sci. USA* 83, 8122–8126.

Fuller, A.O., and Spear, P.G. (1987). Anti-glycoprotein D antibodies that permit adsorption but block infection by herpes simplex virus 1 prevent virion-cell fusion at the cell surface. *Proc. Natl. Acad. Sci. USA* 84, 5454–5458.

Gournier, H., Goley, E.D., Niederstrasser, H., Trinh, T., and Welch, M.D. (2001). Reconstitution of human Arp2/3 complex reveals critical roles of individual subunits in complex structure and activity. *Mol. Cell* 8, 1041–1052.

Gruenheid, S., and Finlay, B.B. (2003). Microbial pathogenesis and cytoskeletal function. *Nature* 422, 775–781.

Gundlach, B.R. et al. (1997). Construction, replication, and immunogenic properties of a simian immunodeficiency virus expressing interleukin-2. *J. Virol.* 71, 2225–2232.

Harlander, R.S., Way, M., Ren, Q., Howe, D., Grieshaber, S.S., and Heinzen, R.A. (2003). Effects of ectopically expressed neuronal Wiskott-Aldrich syndrome protein domains on *Rickettsia rickettsii* actin-based motility. *Infect. Immun.* 71, 1551–1556.

Higgs, H.N., Blanchoin, L., and Pollard, T.D. (1999). Influence of the C terminus of Wiskott-Aldrich syndrome protein (WASP) and the Arp2/3 complex on actin polymerization. *Biochemistry* 38, 15212–15222.

Higgs, H.N., and Pollard, T.D. (2001). Regulation of actin filament network formation through ARP2/3 complex: activation by a diverse array of proteins. *Annu. Rev. Biochem.* 70, 649–676.

Ichihashi, Y., and Oie, M. (1996). Neutralizing epitope on penetration protein of vaccinia virus. *Virology* 220, 491–494.

Iyengar, S., Hildreth, J.E., and Schwartz, D.H. (1998). Actin-dependent receptor colocalization required for human immunodeficiency virus entry into host cells. *J. Virol.* 72, 5251–5255.

Kizhatil, K., and Albritton, L.M. (1997). Requirements for different components of the host cell cytoskeleton distinguish ecotropic murine leukemia virus entry via endocytosis from entry via surface fusion. *J. Virol.* 71, 7145–7156.

Krause, M., Sechi, A.S., Konradt, M., Monner, D., Gertler, F.B., and Wehland, J. (2000). Fyn-binding protein (Fyb)/SLP-76-associated protein (SLAP), Era/vasodilator-stimulated phosphoprotein (VASP) proteins and the Arp2/3 complex link T cell receptor (TCR) signaling to the actin cytoskeleton. *J. Cell Biol.* 149, 181–194.

Li, E., Stupack, D., Bokoch, G.M., and Nemerow, G.R. (1998). Adenovirus endocytosis requires actin cytoskeleton reorganization mediated by Rho family GTPases. *J. Virol.* 72, 8806–8812.

Locker, J.K., Kuehn, A., Schleich, S., Rutter, G., Hohenberg, H., Wepf, R., and Griffiths, G. (2000). Entry of the two infectious forms of vaccinia virus at the plasma membrane is signaling-dependent for the IMV but not the EEV. *Mol. Biol. Cell* 11, 2497–2511.

Machesky, L.M., and Insall, R.H. (1998). Scar1 and the related Wiskott-Aldrich syndrome protein, WASP, regulate the actin cytoskeleton through the Arp2/3 complex. *Curr. Biol.* 8, 1347–1356.

Machesky, L.M., Mullins, R.D., Higgs, H.N., Kaiser, D.A., Blanchoin, L., May, R.C., Hall, M.E., and Pollard, T.D. (1999). Scar, a WASp-related protein, activates nucleation of actin filaments by the Arp2/3 complex. *Proc. Natl. Acad. Sci. USA* 96, 3739–3744.

Maddon, P.J., McDougal, J.S., Clapham, P.R., Dalgleish, A.G., Jamal, S., Weiss, R.A., and Axel, R. (1988). HIV infection does not require endocytosis of its receptor, CD4. *Cell* 54, 865–874.

- Marchand, J.B., Kaiser, D.A., Pollard, T.D., and Higgs, H.N. (2001). Interaction of WASP/Scar proteins with actin and vertebrate Arp2/3 complex. *Nat. Cell Biol.* 3, 76–82.
- May, R.C., Caron, E., Hall, A., and Machesky, L.M. (2000). Involvement of the Arp2/3 complex in phagocytosis mediated by FcγR or CR3. *Nat. Cell Biol.* 2, 246–248.
- McClure, M.O., Sommerfelt, M.A., Marsh, M., and Weiss, R.A. (1990). The pH independence of mammalian retrovirus infection. *J. Gen. Virol.* 71, 767–773.
- McDonald, D., Vodicka, M.A., Lucero, G., Svitkina, T.M., Borisy, G.G., Emerman, M., and Hope, T.J. (2002). Visualization of the intracellular behavior of HIV in living cells. *J. Cell Biol.* 159, 441–452.
- McGee, K., Zettl, M., Way, M., and Fallman, M. (2001). A role for N-WASP in invasin-promoted internalisation. *FEBS Lett.* 509, 59–65.
- Miki, H., Miura, K., and Takenawa, T. (1996). N-WASP, a novel actin-depolymerizing protein, regulates the cortical cytoskeletal rearrangement in a PIP2-dependent manner downstream of tyrosine kinases. *EMBO J.* 15, 5326–5335.
- Miki, H., and Takenawa, T. (1998). Direct binding of the verprolin-homology domain in N-WASP to actin is essential for cytoskeletal reorganization. *Biochem. Biophys. Res. Commun.* 243, 73–78.
- Moreau, V., Frischknecht, F., Reckmann, I., Vincentelli, R., Rabut, G., Stewart, D., and Way, M. (2000). A complex of N-WASP and WIP integrates signalling cascades that lead to actin polymerization. *Nat. Cell Biol.* 2, 441–448.
- Nussbaum, O., Broder, C.C., and Berger, E.A. (1994). Fusogenic mechanisms of enveloped-virus glycoproteins analyzed by a novel recombinant vaccinia virus-based assay quantitating cell fusion-dependent reporter gene activation. *J. Virol.* 68, 5411–5422.
- Nussbaum, O., Roop, A., and Anderson, W.F. (1993). Sequences determining the pH dependence of viral entry are distinct from the host range-determining region of the murine ecotropic and amphotropic retrovirus envelope proteins. *J. Virol.* 67, 7402–7405.
- Panchal, S.C., Kaiser, D.A., Torres, E., Pollard, T.D., and Rosen, M.K. (2003). A conserved amphipathic helix in WASP/Scar proteins is essential for activation of Arp2/3 complex. *Nat. Struct. Biol.* 10, 591–598.
- Pantaloni, D., Le Clainche, C., and Carlier, M.F. (2001). Mechanism of actin-based motility. *Science* 292, 1502–1506.
- Ragheb, J.A., and Anderson, W.F. (1994). pH-independent murine leukemia virus ecotropic envelope-mediated cell fusion: implications for the role of the R peptide and p12E TM in viral entry. *J. Virol.* 68, 3220–3231.
- Rietdorf, J., Ploubidou, A., Reckmann, I., Holmstrom, A., Frischknecht, F., Zettl, M., Zimmermann, T., and Way, M. (2001). Kinesin-dependent movement on microtubules precedes actin-based motility of vaccinia virus. *Nat. Cell Biol.* 3, 992–1000.
- Robinson, R.C., Turbedsky, K., Kaiser, D.A., Marchand, J.B., Higgs, H.N., Choe, S., and Pollard, T.D. (2001). Crystal structure of Arp2/3 complex. *Science* 294, 1679–1684.
- Rohatgi, R., Ma, L., Miki, H., Lopez, M., Kirchhausen, T., Takenawa, T., and Kirschner, M.W. (1999). The interaction between N-WASP and the Arp2/3 complex links Cdc42-dependent signals to actin assembly. *Cell* 97, 221–231.
- Rosenthal, K.S., Perez, R., and Hodnuchak, C. (1985). Inhibition of herpes simplex virus type 1 penetration by cytochalasin B and D. *J. Gen. Virol.* 66, 1601–1605.
- Rozelle, A.L. *et al.* (2000). Phosphatidylinositol 4,5-bisphosphate induces actin-based movement of raft-enriched vesicles through WASP-Arp2/3. *Curr. Biol.* 10, 311–320.
- Sakamoto, T., Ushijima, H., Okitsu, S., Suzuki, E., Sakai, K., Morikawa, S., and Muller, W.E. (2003). Establishment of an HIV cell-cell fusion assay by using two genetically modified HeLa cell lines and reporter gene. *J. Virol. Methods* 114, 159–166.
- Sakisaka, T. *et al.* (2001). Requirement of interaction of nectin-1α/HveC with afadin for efficient cell-cell spread of herpes simplex virus type 1. *J. Virol.* 75, 4734–4743.
- Scaplehorn, N., Holmstrom, A., Moreau, V., Frischknecht, F., Reckmann, I., and Way, M. (2002). Grb2 and Nck act cooperatively to promote actin-based motility of vaccinia virus. *Curr. Biol.* 12, 740–745.
- Smith, G.L., Vanderplasschen, A., and Law, M. (2002). The formation and function of extracellular enveloped vaccinia virus. *J. Gen. Virol.* 83, 2915–2931.
- Stein, B.S., Gowda, S.D., Lifson, J.D., Penhallow, R.C., Bensch, K.G., and Engleman, E.G. (1987). pH-independent HIV entry into CD4-positive T cells via virus envelope fusion to the plasma membrane. *Cell* 49, 659–668.
- Takase-Yoden, S., and Watanabe, R. (1999). Contribution of virus-receptor interaction to distinct viral proliferation of neuropathogenic and nonneuropathogenic murine leukemia viruses in rat glial cells. *J. Virol.* 73, 4461–4464.
- Takenawa, T., and Miki, H. (2001). WASP and WAVE family proteins: key molecules for rapid rearrangement of cortical actin filaments and cell movement. *J. Cell Sci.* 114, 1801–1809.
- Urano, T., Liu, J., Zhang, P., Fan, Y., Egile, C., Li, R., Mueller, S.C., and Zhan, X. (2001). Activation of Arp2/3 complex-mediated actin polymerization by cortactin. *Nat. Cell Biol.* 3, 259–266.
- Vanderplasschen, A., Hollinshead, M., and Smith, G.L. (1998). Intracellular and extracellular vaccinia virions enter cells by different mechanisms. *J. Gen. Virol.* 79, 877–887.
- Wang, K., Huang, S., Kapoor-Munshi, A., and Nemerow, G. (1998). Adenovirus internalization and infection require dynamin. *J. Virol.* 72, 3455–3458.
- Weaver, A.M., Karginov, A.V., Kinley, A.W., Weed, S.A., Li, Y., Parsons, J.T., and Cooper, J.A. (2001). Cortactin promotes and stabilizes Arp2/3-induced actin filament network formation. *Curr. Biol.* 11, 370–374.
- Weaver, A.M., Young, M.E., Lee, W.L., and Cooper, J.A. (2003). Integration of signals to the Arp2/3 complex. *Curr. Opin. Cell Biol.* 15, 23–30.
- Weed, S.A., Karginov, A.V., Schafer, D.A., Weaver, A.M., Kinley, A.W., Cooper, J.A., and Parsons, J.T. (2000). Cortactin localization to sites of actin assembly in lamellipodia requires interactions with F-actin and the Arp2/3 complex. *J. Cell Biol.* 151, 29–40.
- Weed, S.A., and Parsons, J.T. (2001). Cortactin: coupling membrane dynamics to cortical actin assembly. *Oncogene* 20, 6418–6434.
- Welch, M.D., Rosenblatt, J., Skoble, J., Portnoy, D.A., and Mitchison, T.J. (1998). Interaction of human Arp2/3 complex and the *Listeria monocytogenes* ActA protein in actin filament nucleation. *Science* 281, 105–108.
- Wittels, M., and Spear, P.G. (1991). Penetration of cells by herpes simplex virus does not require a low pH-dependent endocytic pathway. *Virus Res.* 18, 271–290.
- Zalavsky, J., Grigorova, I., and Mullins, R.D. (2001). Activation of the Arp2/3 complex by the *Listeria acta* protein. Acta binds two actin monomers and three subunits of the Arp2/3 complex. *J. Biol. Chem.* 276, 3468–3475.
- Zhang, J. *et al.* (1999). Antigen receptor-induced activation and cytoskeletal rearrangement are impaired in Wiskott-Aldrich syndrome protein-deficient lymphocytes. *J. Exp. Med.* 190, 1329–1342.
- Zhang, J., Shi, F., Badour, K., Deng, Y., McGavin, M.K., and Siminovich, K.A. (2002). WASP verprolin homology, cofilin homology, and acidic region domain-mediated actin polymerization is required for T cell development. *Proc. Natl. Acad. Sci. USA* 99, 2240–2245.

Editor-Communicated Paper

Role of Follicular Dendritic Cells in the Early HIV-1 Infection: *In vitro* Model without Specific Antibody

Midori Taruishi¹, Kazuo Terashima¹, Md. Zahidunnabi Dewan¹, Norio Yamamoto¹, Satoshi Ikeda², Daisuke Kobayashi², Yoshinobu Eishi², Momoko Yamazaki³, Tohru Furusaka⁴, Masahiro Sugimoto⁵, Masanori Ishii³, Ken Kitamura⁶, and Naoki Yamamoto^{*1}

Departments of ¹Molecular Virology, Bio-Response, and ²Human Pathology, Graduate School, Tokyo Medical and Dental University, Bunkyo-ku, Tokyo 113–8519, Japan, ³Division of Otorhinolaryngology, Tokyo Kosei-Nenkin Hospital, Shinjuku-ku, Tokyo 162–8543, Japan, ⁴Division of Otorhinolaryngology, Nihon University Surugadai Hospital, Chiyoda-ku, Tokyo 101–8309, Japan, ⁵Division of Otorhinolaryngology, Sanraku Hospital, Chiyoda-ku, Tokyo 101–0062, Japan, ⁶Department of Otorhinolaryngology, Graduate School, Tokyo Medical and Dental University, Bunkyo-ku, Tokyo 113–8519, Japan

Communicated by Dr. Hidechika Okada: Received June 29. Accepted July 12

Abstract: About 90% of HIV-1 RNA in the lymph nodes is reported to localize in follicular dendritic cells-network (FDC-NW) as early as several days after infection and as much as that in the late stage. But the mechanism remains to be fully understood. To elucidate the role of follicular dendritic cells (FDC) in the early stage of HIV-1 infection, FDC-like cell strains (FDCLC) were established and they were characterized in the co-culture system with T cells for their effect on HIV-1 trapping and replication in p24 immunoassay, immunohistochemistry as well as confocal and electronmicroscopy. Established FDCLC were positive for CNA-42, S-100 α and intercellular desmosome-like junctions. L-SIGN and DC-SIGN were also detected in FDCLC. Alu-HIV-1 PCR analysis showed no HIV-1 integration in FDCLC. FDCLC trapped HIV-1 and transferred them to uninfected MOLT-4 T cells (MOLT-4) efficiently in the absence of specific antibody. FDCLC also accelerated HIV-1 replication in HIV-1-pre-exposed MOLT-4. These unique FDCLC effects were explained, at least partly, by the fact that FDCLC up-regulated CD4 expression in MOLT-4 and helped T cells escape from apoptosis in the co-culture. These data suggest that FDC/FDCLC engage not only in trapping but also in active expansion of HIV-1 in the absence of specific antibody.

Key words: HIV-1, FDC, GC, L-SIGN

HIV-1 epidemic does not cease in the developed countries despite of highly active antiretroviral therapy (HAART) while it becomes more and more catastrophic in the developing countries, especially in Africa and Asia. For this reason, new strategies are anticipated not only from medical but also from social aspects (15). The hereto-prevalled therapy depends upon interference with the steps of viral reverse transcription and maturation in the major target cells such as CD4 T cells and macrophages. But as yet, little attention has been paid so far to the most inflamed lesion; that is, germinal cen-

ters (GC) of lymphoid tissues (2, 8, 16, 20, 29), scattering in the whole body. Immunodeficiency in AIDS is probably the results of not only depletion of CD4 T cells but more importantly of abolishment of the GC function as represented by “follicle lysis” or destruction of the FDC-NW (14). FDC plays a key role in the sec-

*Address correspondence to Dr. Naoki Yamamoto, Department of Molecular Virology, Bio-Response, Graduate School, Tokyo Medical and Dental University, 1–5–45, Yushima, Bunkyo-ku, Tokyo 113–8519, Japan. Fax: +81–3–5803–0124. E-mail: yamamoto.mmb@tmd.ac.jp

Abbreviations: CR1, complement receptor 1; DC, dendritic cells; DC-SIGN, DC-specific intercellular adhesion molecule (ICAM)-3-grabbing nonintegrin; FDC, follicular dendritic cells; FDCLC, FDC-like cell strains; FDC-NW, FDC-network; GC, germinal centers; HAART, highly active antiretroviral therapy; HIV-1, human immunodeficiency virus type 1; L-SIGN, liver endothelial cell-specific intercellular adhesion molecule (ICAM)-3-grabbing nonintegrin; MoAb and PolyAb, monoclonal and polyclonal antibodies; TCID₅₀, 50% tissue culture-infectious dose.

ondary immune response (24). Unlike dendritic cells (DC), FDC, localizing in GC, trap antigens including HIV-1 on their outer-surface for a long-term in a form of immune complex unprocessed or infective (16, 29). Following booster stimulation, FDC-NW is transiently loosened resulting in reversible follicle lysis and release of the antigens as ICCOSOMES (23) to be taken by B cells in GC to present them to T cells eventually. In HIV-1 infection, repeated waves of viremic attacks and over-load of the immune complex possibly lead to irreversible follicle lysis due to damage of FDC-NW. The majority (98%) of HIV-1 RNA in the lymph nodes accumulates in FDC-NW (18). In spite of successful HAART regimen with more than 2,500-fold RNA reduction in the virus pool, HIV-1 in some FDC-NW remained infective giving rise to viral variants (18) and accelerating HIV-1 infection in the neighboring T cells (20). Elaborate clinical follow-up studies evidenced HIV-1 accumulated in FDC-NW as early as a few days after acute retroviral symptom (median duration; 7 days) even in the absence of specific antibody (8, 16). Stoiber et al. (19) explained that HIV-1 of itself could be trapped on complement receptor 1 (CR1) of FDC via C1q coated on HIV-1 because of molecular mimicry of gp41 to CR1. HIV-1 trapped in FDC-NW in the early clinical stage certainly contributes to further HIV-1 infection by T cells in GC and may soon be a new target of anti-HIV-1 strategy.

Using an *in vitro* model with newly isolated FDCLC, we attempted to clarify the mechanism by which HIV-1 was trapped by FDC without specific antibody or active complement and FDC involved in rapid and vigorous HIV-1 replication by co-existing T cells. We demonstrated here that FDC-NW was not only a reservoir of HIV-1 but also a potent amplifier of the infected cells from the initial stage of HIV-1 infection.

Materials and Methods

Isolation and culture of human FDC. FDCLC were isolated from fresh palatine tonsils, surgically-removed under informed consents of patients according to the university ethic committee. Tonsils were cut into pieces 2–3 mm thick and then digested for 15 min at 37 C with collagenase (type I, Wako, Tokyo). Following rinsing with RPMI-1640 (Sigma) by centrifugation at 400×g for 7 min, cells were filtered through a φ70 μm nylon mesh and over-layered on a 1.25, 2.5 and 5% continuous BSA gradient at 1×g for 2 hr. The lowest fraction with a higher density fraction was re-suspended and cultured in RPMI-1640 medium plus 10% FCS (25). Cell clusters in the lowest fraction included cells positive for DRC-1, a specific MoAb to FDC. One

week after the culture, adherent spindle-shaped FDCLC appeared from the cell clusters after having released lymphoid cells and spontaneously proliferated without additional cytokines or growth factors. FDCLC were split every 4 to 5 days at 1:2 to 1:3 by replating with 0.5% trypsin + 1 mM EDTA.

Immunohistochemistry. Following centrifugation at 1,000 rpm for 5 min with a rotor for plates and removal of the supernatants, cells cultured in 8-well chamber slides (NalgeNunc International) were fixed in acetone for 30 min after drying. Monoclonal and polyclonal antibodies (MoAb and PolyAb), tabulated in Table 1, were used including FDC-specific MoAbs, DRC-1 and CNA-42 as well as MoAb to p24 and PCNA (DAKO). Immunostaining was performed in the indirect method with HRP-labeled goat F_{ab}, anti-mouse Igs (ICN, Ohio, U.S.A.), absorbed with heat-aggregated human plasma-gel, following endogenous peroxidase-inhibition with 0.1% phenylhydrazinium chloride (Wako, Tokyo) and blocking with 5% goat serum. The specimen were colored with DAB solution [0.05% diaminobenzidine-4HCl (Wako)/0.05 M Tris-HCl (PH 6.8) plus 0.003% H₂O₂]. Combination of TUNEL method for apoptosis and immunostaining was performed as previously described (12).

Virus preparation and p24 assay. HIV-1 wild type viral stocks were produced by calcium phosphate transfection of 293T cells with the proviral vector plasmid NL4-3 (X4-tropic strain). Briefly, supernatants of the transfected 293T cell cultures were collected after 24 or 48 hr, filtered through a 0.45 μm pore-sized filter, treated with DNase I (250 U/ml, Sigma) for 30 min at 37 C to inactivate free proviral DNA, and stored at –80 C for further use. P24 in virus stocks or culture medium-samples were assayed with Lumipulse (Fujirebio, Tokyo) and the infectious units were determined using tissue culture-infective dose (TCID₅₀) analyses on MOLT-4. VSV-env GFP tagged pseudovirus HIV-1 were produced by calcium phosphate co-transfection of 293T cells with NL-EGFP and pH CMV VSV-G.

PCR primers and condition. Genomic DNA was isolated from cells (10⁶ cells) with a lysis buffer containing proteinase K. In first PCR, DNA was amplified between Alu sequence in human genome and integrated proviral DNA with following primers (Alu-tag F1; 5'-GGCTGAGGCAGGAGAATGG-3', Alu-tag R1; 5'-CAATATCATAACGCCGAGAGTGCGCGCTTCAGC-AAG-3'). After first PCR, second PCR was carried out using 2 μl of first PCR product as a template with following primers (Alu-tag F2; 5'-TTGTTACACCCTATGAGCCAGC-3', Alu-tag R2; 5'-CAATATCATAACGCCGAGAGTGC-3'). The Alu-tag R2 primer involves some tag sequences, to which Alu-tag R2 primer is

Table 1. Immunochemistry of a FDCLC strain (#48)

MoAb	Specificity	Cell phenotype	Dilutions tested	FDCLCs	Source
R4/23 (DRC-1)	Follicular dendritic cell	FDCs	1:200	-	DAKO, M0709
CNA-42	Follicular dendritic cell	FDCs	1:100	+	DAKO, M7157
D4A3	S-100 α chain	FDCs	1:50	+	Nihon Kotai, 611318
A6H1	S-100 β chain	DCs	1:50	-	Nihon Kotai, 611516
4B12	CD4	T cell, monocytes, macrophages	1:50	-	Novocastra, NCL-CD4-368
TS1/22.1.1.13	CD11a (LFA-1 α)	Leucocytes	1	-	TKG0418
HL3	CD11c	DCs, NK	1:50	-	R&D System, BCA3
1F8	CD21	FDCs, mature B cells	1:50	-	DAKO, M0784
1B12	CD23	FDCs	1:50	-	Novocastra, NCL-CD23-1B12
G28.5	CD40	B cells, fibroblasts, FDCs	1	+	TKG0520
1.22/4.14	CD45	Leucocytes	1:50	-	Nichirei, 412961
11c8I	CD54	Monocytes, fibroblasts, endothelia	1:50	+	R&D System, BBA3
32.2	CD64	DCs, monocytes	1	+	TKG0522
DCN46	CD209	DCs	1:50	+	BD, 551186
120507	CD209	DCs	1:50	+	R&D System, MAB161
120604	CD209L	Endothelia in liver and lymph nodes	1:50	+	R&D System, MAB162
L243	MHC II		1	-	TKG0425
HR2	Acetylcholinesterase	Cerebellum	1:50	+	Novocastra, NCL-AChE
5B5	Fibroblast	Fibroblasts	1:50	+	DAKO, M0877
IVR7	CXCR4		1:50	+	Gift from Prof. T. Uchiyama
AI58	CXCR4		1:50	+	Gift from Prof. T. Uchiyama
THS123	CXCR4		1:50	+	Gift from Prof. T. Uchiyama

designed to fit. Irrespective of integration sites of HIV into host cell genome, about 550 base pair-long DNA fragments are amplified and could be detected as a single band in agarose electrophoresis. PCR for beta globin gene was performed with BGF (5'-CAAGAAAGT-GCTCGGTGCCTT-3') and BGR (5'-CCTGAAGTT-CTCAGGATCCACG-3') primers as a loading control.

In situ hybridization. FDCLC cultured in 8-well slide chambers and fresh frozen sections, 10 μ m thick, of tonsils were fixed in 4% paraformaldehyde. *In situ* hybridization was performed (3, 27) using GenePoint System (K0620, DAKO) according to manufacturer's protocol. Specimens were first treated with 1% pepsin/0.01 N HCl at 37 C for 10 min and washed DEPC. They were re-fixed in 4% PFA. After treatment with 0.1 M TEA/0.25% acetic anhydride at RT for 10 min and washing in PBS/DEPC, specimens were dehydrated with 100% ethanol twice and dried. Hybridization was performed with hybridization solution at 42 C for 16 hr. The solution contained 18 μ l DAKO buffer and 2 μ l DC-SIGN or L-SIGN probes: (5'-GCTGAGGAGCAG-AACTTCCTACAGCTGCAGT-3' or 5'-CCAGAACCT-GACCCAGCTTAAAGCTGCAGT-3') previously described for Southern blotting probes (13).

Transmission of HIV-1 from FDCLC to MOLT-4 cells. 2.5–10.0 \times 10⁴ FDCLC and control cells were cultured in 24 or 48-well dishes for 2 or 3 days. After exposure to HIV-1 (NL4-3) with MOI 0.5 at 37 C for 2 hr and rinsing twice with PBS, the cells were cultured in

new medium for several days. Following removal of the supernatants and addition of MOLT-4 (5.0 \times 10⁴ cells), p24 in the supernatant were measured 7 days after. In some experiments FDCLC were co-cultured with MOLT-4 via a membrane with pores 0.4 μ m in diameter (Transwell, Corning Costar, N.Y., U.S.A.).

Co-culture with HIV-1-infected MOLT-4 cells and FDCLC. 2.5–10.0 \times 10⁴ FDCLC and control cells including HepG2 and MRC-5 (fibroblast cell line) were cultured in 24 or 48-well dishes for 2 or 3 days. MOLT-4 exposed to HIV-1 (NL4-3) at 37 C for 2 hr and rinsed with PBS twice were cultured alone or co-cultured with FDCLC or control cells. P24 antigen levels were measured 7 days in their supernatants. Co-culture experiments via the membrane were also performed as described above.

Electron microscopy. Cells cultured in 24-well plates at 5 \times 10⁴ cells/well in a total volume of 1 ml were fixed in 1.25% glutaraldehyde (TAAB, U.K.) for 1 hr followed by 3.0% osmium tetroxide, dehydrated in ethanol and embedded in Epon 812. Uranyl acetate and lead citrate-stained ultrathin sections were examined in transmission electronmicroscopy (H-7100, HITACHI).

Results

Establishment and Characterization of FDCLC in Long-Term Culture Conditions

FDCLC isolated from fresh normal tonsillar tissues

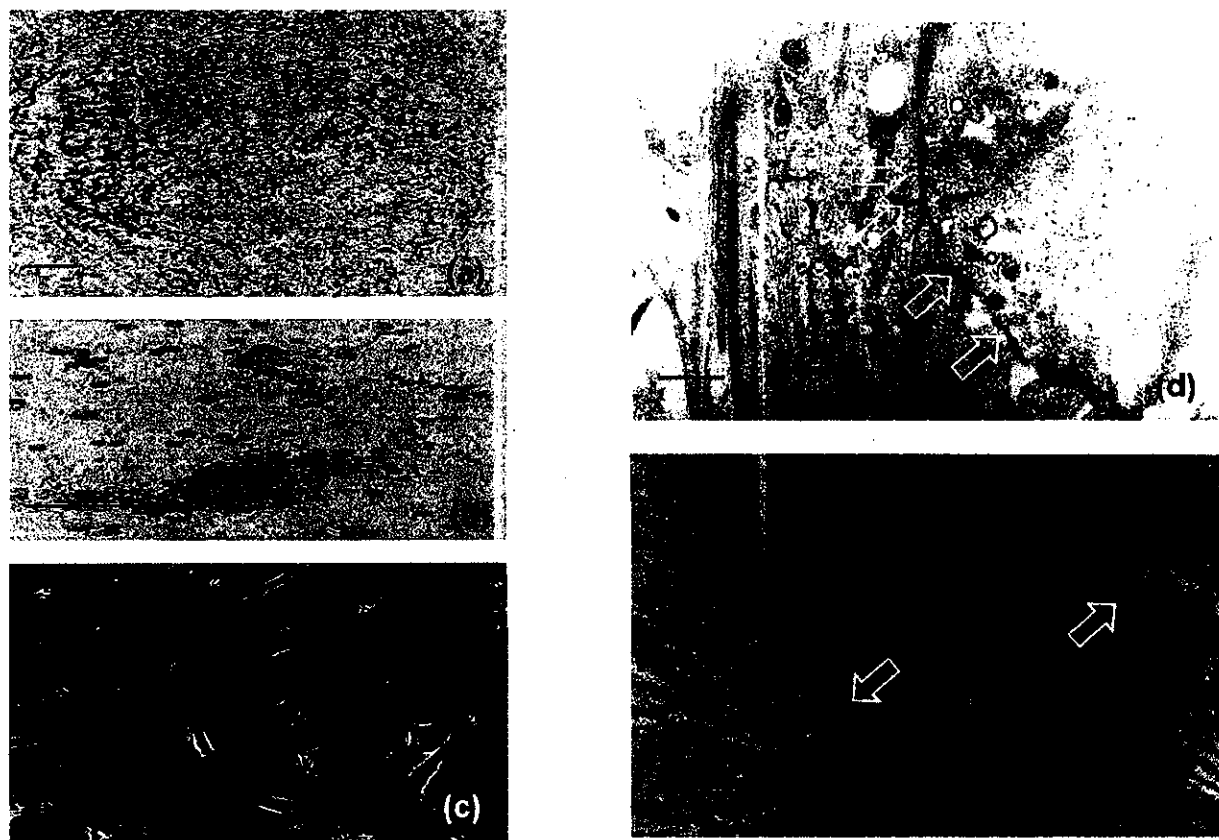


Fig. 1. Isolation and characterization of FDCLC. (a) Immunohistochemistry revealed that MoAb DRC-1 stained the FDC-NW in germinal center of tonsil. (b) DRC-1-positive cells in the cell clusters of BSA-gradient fraction (Cytospin specimen of FDCLC). (c) A phase contrast-image of FDCLC. The bar indicates 100 μ m. Electron microscopy disclosed FDCLC were of FDC. (d) Arrows indicate desmosome-like junctions. (e) Elongated fili-form cytoplasmic extensions (white arrows) and collagen fibers (black arrows). The bar indicates 1 μ m.

proliferated extending cytoplasmic projections varying in length and branch and have been kept growing for more than one year (Fig. 1, (a)–(c)). Eventually 10 FDCLC strains were established and the following data were mainly obtained with a representative FDCLC strain #48. FDCLC were elongated, rather eukaryonic cells sometimes with plural nuclei and characterized by abundant fili-form cytoplasmic extensions, tangled, and desmosome-like junctions (Fig. 1 (d)). Collagen fibers ran along their long axis extracellularly (Fig. 1 (e)).

In immunostaining, FDCLC were positive for DRC-1, CD21, CD23 and HLA-DR on the cell membrane initially but became negative soon after *in vitro* culture, while CNA-42, S-100 α , CD54 (ICAM-1) and a fibroblast marker or human prolyl 4-hydroxylase remained positive (Table 1). CD40, CD64 and CXCR4 were weakly positive. CD11c, S-100 β and CD4, markers for DCs, were negative. L-SIGN and DC-SIGN were also positive though the former was rather intensely expressed than the latter (Fig. 2, (a)–(c)). Expression of these markers was also affirmed by *in situ* hybridization

(Fig. 2, (d)–(f)). Fresh-frozen sections of the tonsils confirmed that FDC were positive for L-SIGN and DC-SIGN in single and double immunostaining albeit their expression level varied according to GC and was not so high as seen in DC and related cells (Fig. 2, (g)–(i)). CD11c, S-100 β and CD4 were negative. In addition, FDCLC and MRC-5 showed active production of IL-6 whereas MOLT-4 and HepG2 did not (data not shown). These data indicate that FDCLC sustain morphological and immunological phenotype of FDC.

FDCLC Do Not Allow HIV-1 Integration, but Substantially Trap, Maintain and Transmit HIV-1 to T-Cells in the Absence of Antibody

FDCLC showed no increase in p24 level even 6 days after exposure to NL4-3 (data not shown). To study whether FDCLC permit HIV-1 integration, a new PCR method was devised to detect only integrated HIV-1 DNA. The DNA extracts from FDCLC showed no amplified DNA specific for HIV-1, indicating that HIV-1 DNA was not integrated in these cells. The amplified